

**EVALUATION OF CONFINED LAP-SPLICE CONNECTION
FOR PRECAST CONSTRUCTION**

by

JOHN JOSEPH MYERS, B.A.E.

THESIS

Presented to the Faculty of the Graduate School of

The University of Texas at Austin

in Partial Fulfillment

of the Requirements

for the Degree of

MASTER OF SCIENCE IN ENGINEERING

THE UNIVERSITY OF TEXAS AT AUSTIN

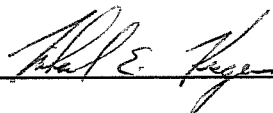
May 1994

Copyright
by
John Joseph Myers
1994

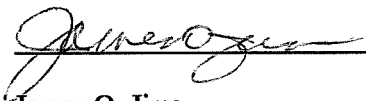
**EVALUATION OF CONFINED LAP-SPLICE CONNECTION
FOR PRECAST CONSTRUCTION**

APPROVED BY

SUPERVISING COMMITTEE:



Michael E. Kreger



James O. Jirsa

DEDICATION

To my Parents, Brother, and Sisters for their love and support my entire life and to the memory of my uncle, Frank A. Talarico Sr.

ACKNOWLEDGEMENT

The author would like to express his deepest thanks to Dr. Michael E. Kreger for friendship, continuous guidance, and suggestions in planning, conducting, and reporting this research effort. In addition, special thanks to Dr. James O. Jirsa for his constructive comments and encouragement during the planning, testing, and written phases of this research.

Sincere thanks to the faculty of the Department of Civil Engineering at The University of Texas at Austin, with special thanks and gratitude to Dr. Ramon Carrasquillo for his support and tremendous generosity during the author's entire career at the university.

The author would also like to express his gratitude for the assistance and cooperation of all the staff of the Phil M. Ferguson Structural Engineering Laboratory as well as the very helpful advise, friendship, and assistance of all fellow graduate students including George Arditzoglou, Joe Muscarella, Hongun Park, and Elias Saqan.

In addition special thanks to Dr. and Mrs. Ben Caudle, as well as Brian and Christine Caudle for truly being the author's adopted "Texas" family.

Finally there are no words the author could use to thank his father and mother for their encouragement and great support throughout his entire life. I love you both dearly.

The study described herein was conducted at The University of Texas Phil M. Ferguson Structural Engineering Laboratory at the Balconies Research Facility in Austin, Texas.

John Joseph Myers

April 20, 1994

ABSTRACT

**EVALUATION OF CONFINED LAP-SPLICE CONNECTION
FOR PRECAST CONSTRUCTION**

by

John Joseph Myers, M.S.E.

The University of Texas at Austin, 1994

Supervising Professor: Michael E. Kreger

The need to investigate the use of precast concrete connections is a topic of growing demand. Currently the majority of precast structures utilize "soft" connections such as bearing plate or neoprene pad type connections to resist gravity loads only, with wall panel elements to resist the lateral loads. The development of cost-effective "rigid" (continuous) precast concrete connections which can resist shear, moment, and axial (gravity) loads will allow for the elimination of wall panel elements as the primary lateral-force-resisting system in a structure.

Six specimens were tested to study the effect of different variables on the behavior of a confined lap-splice connection which could be utilized in a precast application. This discussion presents results of a proposed precast connection through the use of load-deformation and load-slip responses. An evaluation and recommendation of the connection is presented based on a strength and serviceability criteria developed within this pilot study.

TABLE OF CONTENTS

	Page
CHAPTER 1 - INTRODUCTION	1
1.1 Statement of Problem	1
1.1.1 General	1
1.1.2 Connections	1
1.2 Objective	2
1.3 Scope	2
1.4 Project Background	3
CHAPTER 2 - BACKGROUND	4
2.1 Precast Structures	4
2.2 Typical Precast Connections	7
2.3 Bond Failures in Concrete	8
2.4 Previous Research	10
2.4.1 Proposed Design Recommendation	10
2.4.2 Current ACI Code Bond/Development	12
CHAPTER 3 - EXPERIMENTAL PROGRAM	14
3.1 Introduction	14
3.2 Specimen Description	14
3.3 Test Variables	15
3.3.1 Reinforcing Size	15
3.3.2 Lap-Splice Length	15
3.3.3 Confinement	16
3.3.4 Non-Shrink Grout Strength	17
3.3.5 Concrete	17
3.3.6 Loading	17
3.4 Specimen Designation	17

3.5	Materials	18
3.5.1	Concrete	18
3.5.2	Non-Shrink Grout	18
3.5.3	Reinforcement	20
3.6	Construction of Specimens	20
3.6.1	Specimen Construction	20
3.6.2	Longitudinal and Transverse Reinforcement	21
3.6.3	Casting of Specimens	21
3.6.4	Non-Shrink Grout Application	24
3.7	Test Frame	28
3.8	Testing Procedure	30
3.8.1	Preparation for Testing	30
3.8.2	Testing	30
3.9	Instrumentation and Data Acquisition	31
3.9.1	Measurement of Displacements	31
3.9.2	Data Acquisition	31
 CHAPTER 4 - PRESENTATION OF EXPERIMENTAL RESULTS		32
4.1	Introduction	32
4.2	Load History	32
4.3	Connection Capabilities	33
4.4	Load Versus Deformation Response	33
4.4.1	Response of Confined Lap-Splice Specimen with #6 Reinforcing Bars	33
4.4.1.1	Specimen 612	34
4.4.1.2	Specimen 615	34
4.4.2	Response of Confined Lap-Splice Specimen with #10 Reinforcing Bars	38
4.4.2.1	Specimen 1024	38
4.5	Bar-Slip Mechanism	39

CHAPTER 5 - EVALUATION OF RESULTS	43
5.1 Introduction	43
5.2 Reflection on Existing Provisions	43
5.3 Comparisons Between Load-Deformation Responses	45
5.4 Serviceability Concerns	46
5.4.1 Serviceability of #6 Reinforcing Bar Splices	49
5.4.2 Serviceability of #10 Reinforcing Bar Splices	49
5.5 Design and Research Implications	51
CHAPTER 6 - SUMMARY AND CONCLUSIONS	52
6.1 Summary	52
6.2 Conclusions	52
6.3 Further Research Needs	53
APPENDIX - EXPERIMENTAL DATA	55
REFERENCES	71
VITA	74

LIST OF TABLES

Table		Page
3.1	Variables Used in Eqn. 3.1	15
3.2	Determination of Required Duct Size	16
3.3	Concrete Mix Design Proportions	18
3.4	Concrete Mix Design Compressive Strengths	18
3.5	Non-Shrink Grout Compressive Strengths	19
4.1	Summary of Load-Response Data	33
5.1	Comparison of Computed Lap Lengths with Minimum Test Lengths	44
5.2	Recommended Tolerable Crack Widths for Reinforced Concrete	47
5.3	Summary of Connection Evaluation	50
A.1	Load-Deformation Response Data - #6 Bar - 12" Lap-Splice	56
A.2	Load-Deformation Response Data - #6 Bar - 15" Lap-Splice	58
A.3	Load-Deformation Response Data - #6 Bar - 19" Lap-Splice	60
A.4	Load-Deformation Response Data - #10 Bar - 24" Lap-Splice	62
A.5	Load-Deformation Response Data - #10 Bar - 32" Lap-Splice	65
A.6	Load-Deformation Response Data - #10 Bar - 41" Lap-Splice	68

LIST OF FIGURES

Figure	Page
2.1 Precast Wall Elements	4
2.2 Precast Roof and Floor Elements	5
2.3 Precast Beams	6
2.4 Column Supports for Precast Beams	6
2.5 Typical "Rigid" Reinforced Concrete Beam to Column Connection	7
2.6 Typical "Rigid" Precast Concrete Beam to Column Connection	8
2.7 Inclination of Bond Stresses	9
2.8 Bond Stresses in Pullout Failure	9
2.9 Splitting Failure	10
2.10 Definition of Transverse Reinforcement, a_{tr} , Orangun et al.	11
2.11 Splitting Bond Failures, Orangun et al.	12
3.1 Schematic of Typical Specimen	14
3.2 Test Designation Key	17
3.3 Reinforcing Bar Patterns	19
3.4 Rebar Yield and Ultimate Stresses	20
3.5 Specimen Dimensions and Reinforcement	20
3.6 Completed Formwork with Inserts	21
3.7 Completed Formwork	22
3.8 Completed Casting of Specimens	22
3.9 Placement of Concrete in Formwork	23
3.10 Grout Mix Set-Up	24
3.11 Paddle Mixing of Non-Shrink Grout	25
3.12 Flowable Non-Shrink Grout Placement In Specimen	26
3.13 Rodding of Non-Shrink Grout	27
3.14 Plan View of the Test Frame	28
3.15 Overall View of the Test Set-Upwith Specimen	29
3.16 Side View of Specimen in Frame	29
3.17 Steel Wedges and Anchor Plate	30
3.18 Dial Gage Measurement Set-Up	31

4.1	Load-Deformation Response, #6 Bar Lap-Splice (Live End)	35
4.2	Load-Deformation Response, #6 Bar Lap-Splice (Dead End)	36
4.3	Live End and Dead End Response Comparison	37
4.4	Test Frame with Teflon Pads for Unrestrained Horizontal Movement	38
4.5	Typical Cracking in Grout at End of Duct	39
4.6	Load-Deformation Response, #10 Bar Lap-Splice (Live End)	40
4.7	Load-Deformation Response, #10 Bar Lap-Splice (Dead End)	41
4.8	Live End and Dead End Response Comparison	42
5.1	Mechanism of Bond Resistance Under Monotonic Loading	48
5.2	Modified Load-Deformation Response, #6 Rebar	49
5.3	Modified Load-Deformation Response, #10 Rebar	50

CHAPTER 1

INTRODUCTION

1.1 STATEMENT OF PROBLEM

1.1.1 General

Since the early 1960's, building costs have increased at a considerably faster rate than industrial products. This is true not only in the United States, but for most industrialized nations. A major reason for high building costs is the substantial amount of site labor involved in the construction process. In order to reduce this cost, construction and erection schedules have generally been shortened. One structural system which was developed to reduce on-site labor costs and which continues to evolve is precast concrete construction. This construction technique can reduce the overall cost of a structure by mass producing standardized columns, beams, floor or roof elements, wall panels etc. in a precast plant. Savings result because standardized structural elements can be fabricated more efficiently in the precasting yard than on-site, and also because the tighter tolerances that are possible in the fabrication process combined with the connection techniques used in the field result in a more efficient erection process which reduces on-site labor costs. The most common use of precast concrete structures today is precast parking garages and low to medium-rise office buildings and hotels.

1.1.2 Connections

It was mentioned earlier that connection techniques play an important role in precast concrete construction. Cast-in-place reinforced concrete structural elements by their very nature are typically joined together by monolithic connections. Two separate members are rarely joined together in the field by some other construction process. However, it is quite the contrary in the case of precast construction. Precast structural systems are typically prefabricated members which are connected on-site to form the finished structure. In both construction methods, connections can be detailed to transmit gravity forces only, or gravity and horizontal forces in addition to bending moments (in other words, continuous connections). In the case of precast concrete structures, continuous connections comparable to monolithic cast-in-place connections can be achieved by appropriate use of special hardware and reinforcing bars to transmit the tension, compression, and shear forces at connections. This type of precast connection is typically referred

to as a "hard" connection. In contrast, connections which resist gravity loads only, for instance, but permit rotations and a limited amount of motion horizontally to relieve time-dependant forces are often referred to as "soft" connections. Typically a large portion of precast concrete structures involve the use of "soft" beam-column connections such as bearing plate or neoprene pad connections, to resist gravity loads, with wall panel elements to resist lateral loads such as wind or ground motion. Details for "hard" connections, which are also referenced to as "rigid" connections, already exist and have been catalogued in a Prestressed Concrete Institute report [15]. Many of these connections are believed to be impractical for today's construction industry because they are labor intensive and because there are scheduling problems associated with different trade organizations that result during fabrication of the connections. There is currently a federally sponsored research program underway in the United States that is developing ductile, moment-resisting connections (continuous connections) using some of the existing hardware that is currently used in "soft" precast connections. With the development of these cost-effective moment-resisting precast connections, wall panel systems may be eliminated as the primary lateral-force-resisting system.

1.2 OBJECTIVE

The study which is described here examines the behavior of lap-splice connections confined by a steel pipe. Although this is only a "pilot" study to examine the feasibility of such a connection, the long-range intent of this work, and perhaps additional future tests, is to replace existing mechanical and grouted bar coupler devices, used for example to splice column bars, with a simpler, less expensive connector. In order to fulfill this objective, six confined lap-splice connections were tested. Strength of the connections as well as deformation characteristics of the connections were used to evaluate connection performance.

1.3 SCOPE

Background related to splicing of reinforcing bars is presented in Chapter Two. A description of the testing program, the test setup, and material properties are described in Chapter

Three. Results and observations from the six tests are presented in Chapter Four, and the test results are evaluated in Chapter Five. A summary and conclusions along with recommendations for further work are presented in Chapter Six.

1.4 PROJECT BACKGROUND

The experimental setup, fabrication, and testing of the confined precast specimens was conducted by the author under the supervision of Dr. Michael E. Kreger, Associate Professor of Civil Engineering at The University of Texas at Austin. Funds for test specimens and the testing frame were provided by The National Science Foundation under grant No. BCR 9122950.

CHAPTER 2 BACKGROUND

2.1 PRECAST STRUCTURES

Due to the high cost of building materials and escalating labor costs, precast concrete construction has continued to develop rapidly in order to provide a more efficient method of construction. A number of types of precast members and assemblies have established themselves in the market place. Though many of these system assemblies and member types are currently not standardized, they are widely available, with somewhat minor local variations. In addition, the precast process provides sufficient adaptability for special shapes which may be produced for a particular project. The repetitive nature of elements utilized in a project allows these units to be produced economically.

A precast structure may involve the use of column, beam, floor or roof elements, and wall panels. A brief discussion of typically utilized elements in the precast industry is presented to familiarize the reader with current "standard" practice. This will help illustrate the need and advantages of a confined lap-splice connection. Currently four typical types of wall panels are generally used. These are shown below in Figure 2.1.

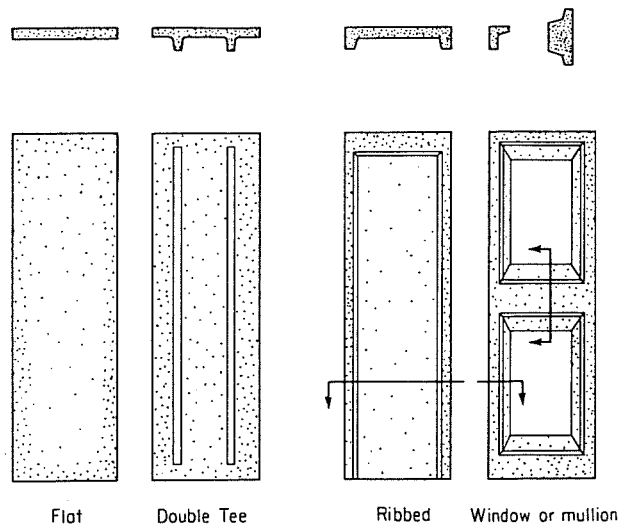


Figure 2.1 Precast Wall Elements [18]

These units are produced in one to four-story high sections and generally in 8 ft widths. In addition, a variety of surface finishes can be produced through the use of exposed aggregate or pigmented cements and admixtures. Stresses in wall panels are quite often more severe during handling and erection than in the finished erected panel. Naturally, the design of the panels must consider the effects of these additional handling / erection stresses on the panel. Another major consideration in panel design, is the control of cracking, primarily for appearance and aesthetics than for safety reasons.

Roof and floor elements are produced in a wide variety of shapes adapted to specific conditions, such as span length, magnitude of load, fire rating, appearance, and other additional factors. Figure 2.2 shows typical examples of common shapes in approximate order of increasing span length.

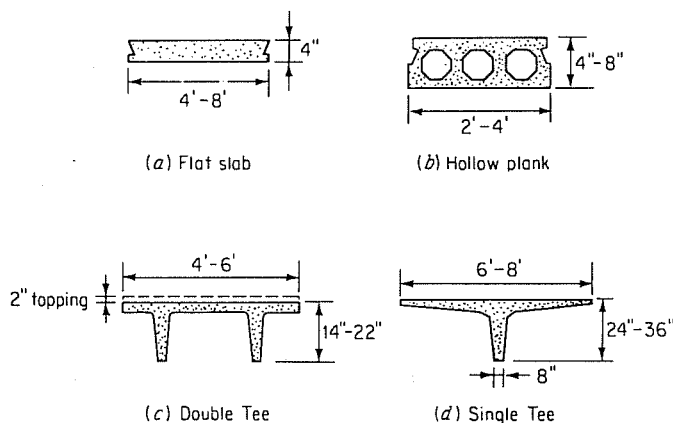


Figure 2.2 Precast Roof and Floor Elements [18]

Floor slabs of precast planks or flat slab units vary both in width and thickness, but generally do not span more than 20 ft, mainly due to the greater efficiency of other types of roof or floor elements. For improved insulation properties and lower plank weight (resulting in increased span potential) hollow precast planks are used. These floor or roof elements may span up to 30 ft with a 2 in. topping slab.

For longer spans, precast double tees are the most widely used shapes. These shapes are generally used for roof spans up to 60 feet. When used as a floor element, a concrete topping of 2 inches is usually applied after the structure is erected to tie the floor elements together. For floors, span lengths of up to 50 ft are generally feasible depending on loading and deflection requirements. Also, precast single tees are available, but are generally used for roof spans.

In the use of precast beams, the type of framing system generally determines the shape of the members. When the roof or floor is supported on the top of a precast beam, most members are rectangular in shape. Quite frequently beams are flush with the top of slab to reduce depth of the structure. This requires a ledge bearing type connection. Figure 2.3 illustrates typical precast beam shapes.

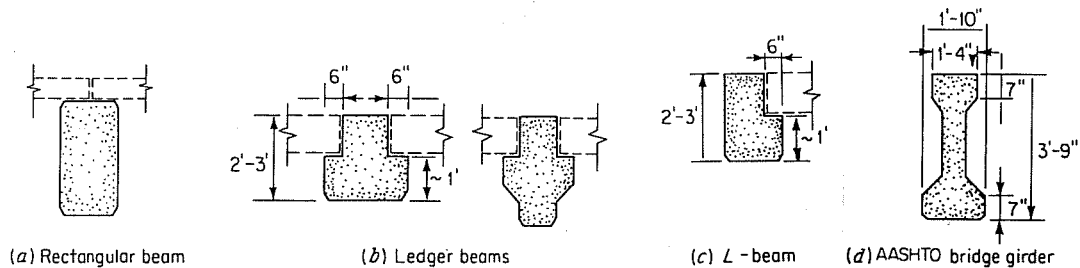


Figure 2.3 Precast Beams [18]

Finally, precast beams are generally supported by columns using one of two approaches. The first is used in single-story applications where the beams physically rest on the top ends of precast columns. It should be noted that the vast number of precast structures have multiple stories. In fact, the confined lap-splice connection is quite suited for connecting columns together in multi-story construction. Currently, corbels are used most commonly to provide supports for precast beams, as depicted in Figure 2.4.

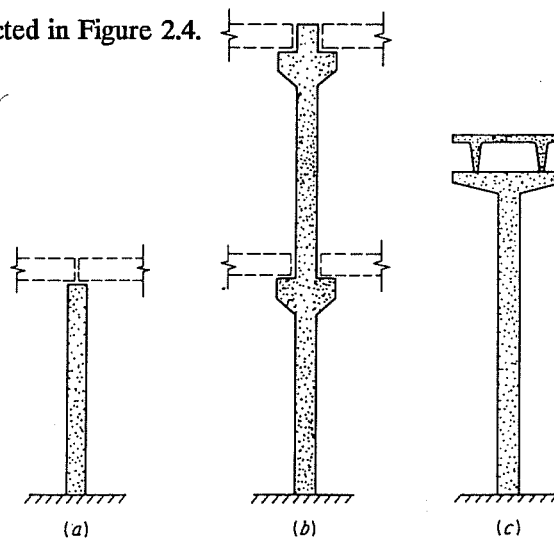


Figure 2.4 Column Supports for Precast Beams [18]

2.2 TYPICAL PRECAST CONNECTIONS

Before being introduced to the proposed confined lap-splice connection, it is important to understand the advantages and disadvantages of current typical precast connections. Typical cast-in-place reinforced concrete structures are commonly considered by their very nature to be monolithic and continuous. Connections between members are typically reinforced, cast-in-place joints. Joining two separate pieces by any other method is rare in this type of construction. On the other hand, precast structures consist of a large number of prefabricated elements which are connected together at the site. While "rigid" connections, which usually result in reinforcement congestion, are somewhat easily detailed in cast-in-place concrete structures (see Figure 2.5), precast concrete connections are typically more difficult to detail and are more labor intensive and expensive. Current practice requires a precast frame to "emulate" cast-in-place construction. Figure 2.6 illustrates an example detailed by PCI [15] to meet such requirements.

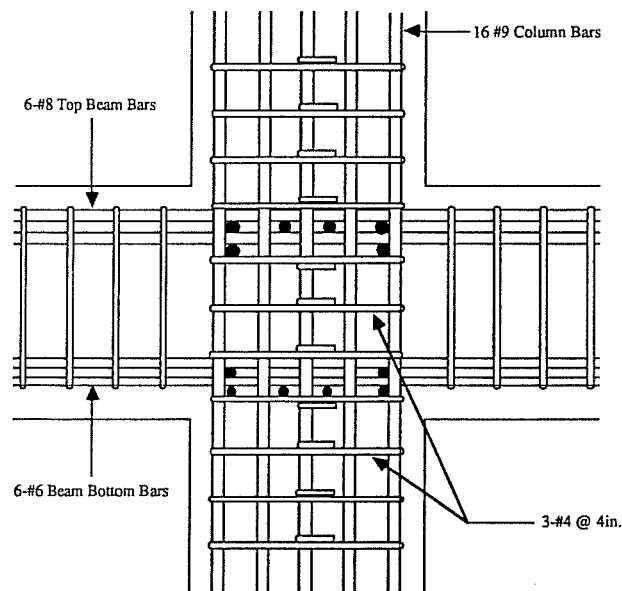


Figure 2.5 Typical "Rigid" Reinforced Concrete Beam to Column Connection [10]

Complexity and expense is a contributing factor to the common use for gravity-load carrying connections, such as beams supported on brackets or corbels, in conjunction with wall panels to resist lateral forces. Gravity-load connections provide little or no continuity or resistance

to moment and uplift at the supports. In this research, the behavior of bars spliced / developed in a steel pipe (hereafter referred to as a "confined lap-splice connection") will be studied. The intent is that such a detail might be used to tie down the ends of a beam, provide continuity of beam steel, or splice column bars.

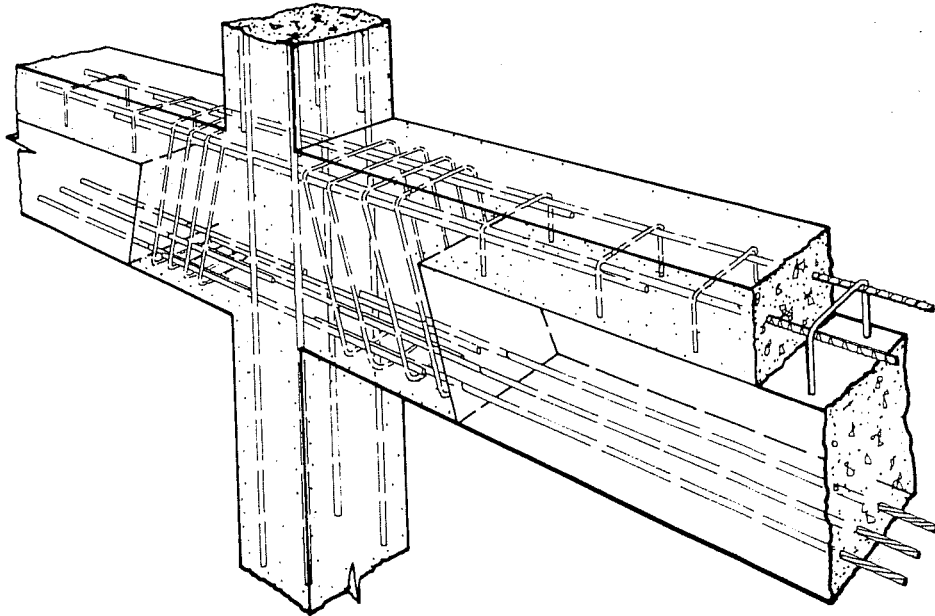


Figure 2.6 Typical "Rigid" Precast Concrete Beam to Column Connection [15]

2.3 BOND FAILURES IN CONCRETE

Bond is the stress that develops at the interface of two materials, in this case steel and concrete, to produce composite action. In reinforced concrete structures, forces are generally transferred to the steel only through the surrounding concrete. The transfer of load or stress from the concrete to steel is made possible by the shearing stresses along the surface between the concrete and embedded steel reinforcing bar. The higher the surface shear or resistance to relative motion or bar slippage under stress, the more effective the interaction between the steel and concrete. The resistance to slippage is called bond or bond stress. Inherent in the analysis of a reinforced concrete section is the assumption that the strain in the concrete and the steel is

equal at the location of the reinforcing steel. This implies a perfect bond between the concrete and steel.

To ensure proper ductility, the bond between the steel and concrete must be maintained until the bars develop 125 percent of yield. The ACI Building Code Requirements for Reinforced Concrete (ACI 318-89) ensures ductility by requiring a development or splice length. The development length is based on the bond strength.

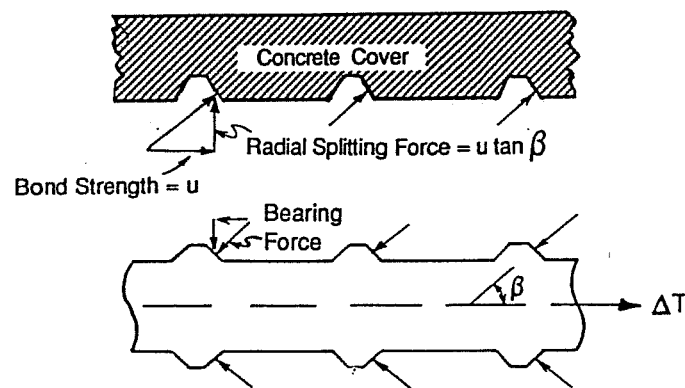


Figure 2.7 Inclination of Bond Stresses [11]

Two modes of failure are commonly recognized, a splitting failure and a pullout failure. In both cases it is assumed that the main component of bond is the reaction of the bar deformations against the surrounding concrete. If the cover and spacing between bars is great enough, or if enough transverse reinforcement is provided, a splitting failure cannot develop and either a pullout failure or yielding of the bar will occur. In a pullout failure, the concrete between bar deformations is sheared from the surrounding concrete (see Figure 2.8). The bond stress for a pullout failure is primarily dependent on the strength of concrete in direct shear. A pullout failure is more likely for small bars or large bars where the depth of cover is large or transverse

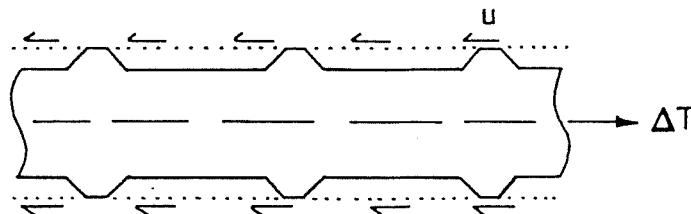


Figure 2.8 Bond Stresses in Pullout Failure [11]

reinforcement is provided around the bar. In both splitting and pullout failure modes the contribution of adhesion to the bond between the bars and concrete is ignored.

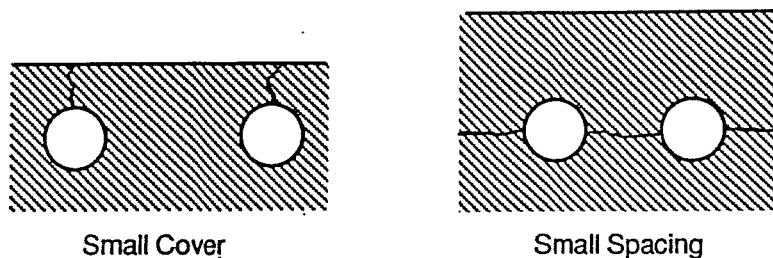


Figure 2.9 Splitting Failure [11]

2.4 PREVIOUS RESEARCH

2.4.1 Proposed Design Recommendation. Due to the special nature of this confined lap-splice connection, the behavior has not been previously researched. Related research has been compiled and comprehensive design recommendations including the effect of confinement have been developed at The University of Texas at Austin. The development length used as a basis for the confined lap-splice application has been based on "A Reevaluation of Test Data on Development Length and Splices" published in ACI by C.O. Orangun, J.O. Jirsa, and J.E. Breen.

This work was based on tests performed in this country and in Europe on the strength of spliced bars confined by transverse reinforcement. The tests included a wide range of transverse steel variables including diameter, spacing, and bar strength. For deformed bars in tension the development length l_d (in inches) shall be computed as the product of the basic development length given by Equation 2.1, but l_d shall be not less than 12 in.

$$l_d = \frac{(10200 d_b)}{\sqrt{f'_c} [1 + 2.5(c/d_b) + K_{tr}] \phi} \quad (2.1)$$

where:

$$\phi = 0.8$$

c - is taken as the lesser of the clear cover over the bar or bars or half the clear spacing between adjacent bars ($c/d_b \leq 2.5$)

$$K_{tr} = (A_{tr} f_y / 600 s d_b) \leq 2.5$$

multiplied by the applicable factor(s) for :

Grade 40 Reinforcement (0.6)

Grade 75 Reinforcement (1.3)

Top Reinforcement (1.3)

Wide Spacing such that $C_x / (C_b d_b) > 3$ (0.9)

Wide Spacing such that $C_x / (C_b d_b) > 6$ (0.7)

Excessive Flexural Reinforcement $(A_{s \text{ REQUIRED}}) / (A_{s \text{ PROVIDED}})$

The basic design equation developed by Orangun has been verified through successful application to tests from various sources.

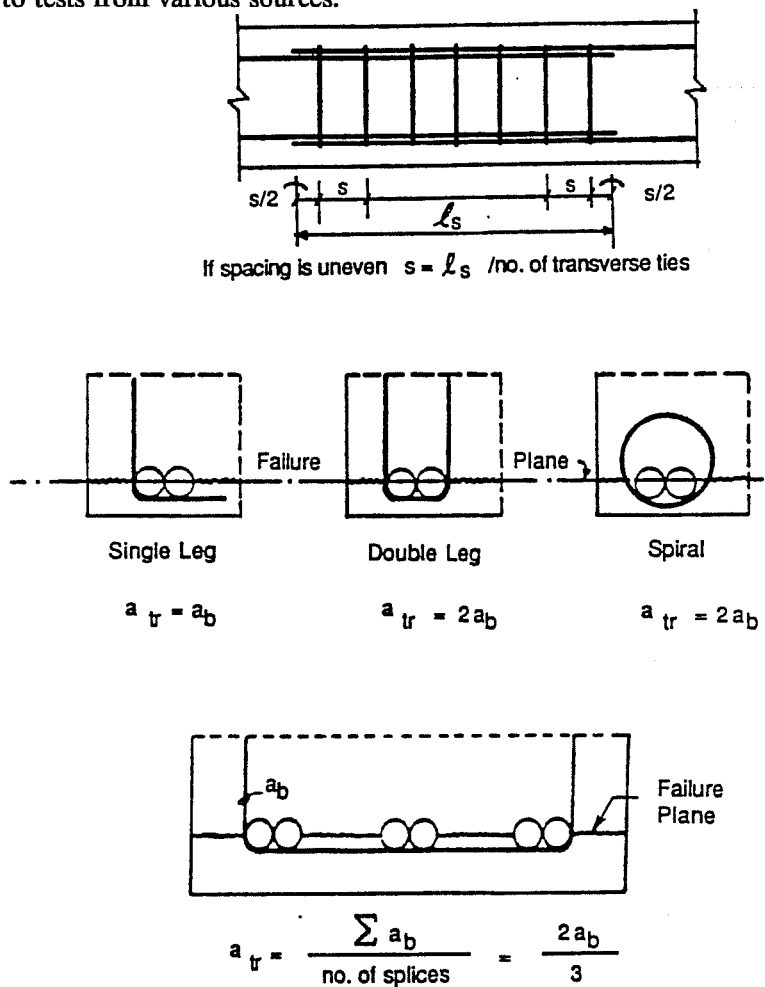


Figure 2.10 Definition of Transverse Reinforcement, a_{tr} , Orangun et al. [14]

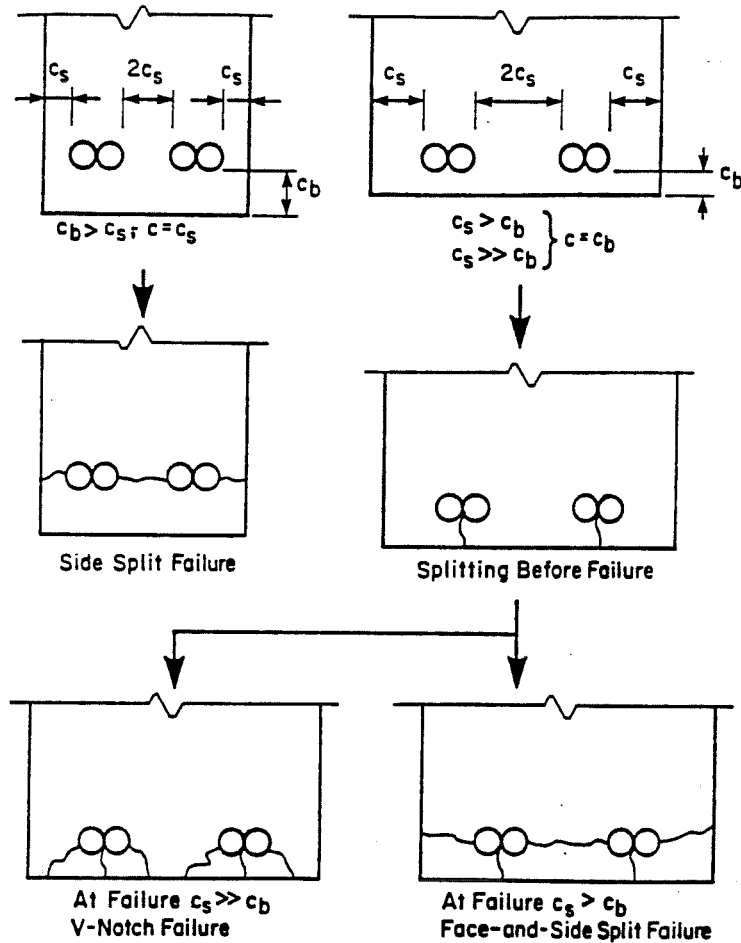


Figure 2.11 Splitting Bond Failures, Orangun et al. [14]

2.4.2 Current ACI Code Bond/Development. Current code provisions (ACI 318-89) also reflect the influence of concrete cover, bar spacing, transverse reinforcement, casting position, and material strengths on splice requirements. The provisions, which are based on the work by Orangun et al., represent the factors listed above with step functions, rather than a continuous function. Splice lengths are the product of a bar basic development length l_{db} and modification factors to reflect cover, bar spacing, etc.

$$l_{db} = \frac{0.04 A_b f_y}{\sqrt{f'_c}} \geq \frac{0.03 d_b f_y}{\sqrt{f'_c}}, \quad \text{where } \sqrt{f'_c} \leq 100 \text{ psi} \quad (2.2)$$

In addition, a lower limit is imposed on the computed development length, l_d , to preclude a pullout failure if sufficient resistance to splitting is provided. The limit, $0.03 d_b f_y / \sqrt{f'_c}$ with $\sqrt{f'_c} \leq 100$ psi is the minimum length required to yield a bar that is subject to pullout. Furthermore, to obtain the splice length, the computed development length, l_d , is multiplied by a factor 1.0 or 1.3 depending on the percentage of steel to be spliced and the stress to be developed.

CHAPTER 3 EXPERIMENTAL PROGRAM

3.1 INTRODUCTION

In this pilot study, six specimens were tested to investigate the behavior of a confined lap-splice connection in tension for a precast concrete application. Variables studied and the nomenclature used for test identification are explained. Material properties, specimen construction, and instrumentation are described along with typical testing procedures.

3.2 SPECIMEN DESCRIPTION

A schematic of a typical specimen is shown in Figure 3.1. The specimen consists of a steel duct which provides confinement for the lap-splice and nominal reinforcement according to Chapter 21 of the ACI 318-89 Building Code [1]. The reinforcement corresponds with nominal longitudinal and transverse reinforcement which would be provided in a seismic design application. The length of the specimens vary based on multiples of a calculated lap-splice length which will be discussed later in this chapter. This configuration is intended to represent an individual lap-splice which would either in precast concrete columns, beams, or panels. During the construction process, prefabricated members would be erected and the lap-splice connection grouted with a flowable grout. In the tests described here, each lap-splice was loaded in tension until failure.

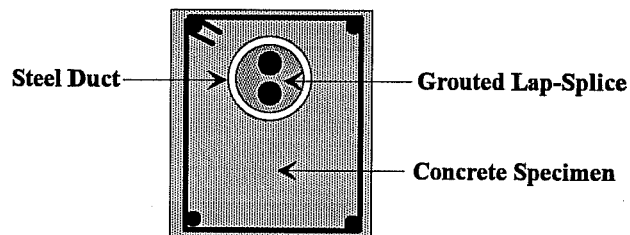


Figure 3.1 Schematic of Typical Specimen

3.3 TEST VARIABLES

The variables studied in this project included :

- 1.) Reinforcement Size
- 2.) Lap-Splice Length
- 3.) Confinement (Duct Diameter and Wall Thickness Varied)

Concrete Strength, Nominal Non-Shrink Grout Strength, and Rebar Steel Strength remained Constant.

3.3.1 Reinforcing Size. Two different reinforcing bar sizes were used in the series of six tests. The two sizes that were used were #6 and #10. These bar sizes were chosen because they represent the range of sizes typically used in precast member applications.

3.3.2 Lap-Splice Length. Three different lap-splice lengths were studied for each rebar size. Lap splice lengths were developed based on the empirical equation developed by Orangun, Jirsa, and Breen [13] which was discussed in Section 2.4. The equation shown again below, includes the effects of confinement. Although the confinement offered by the pipe was substantially greater than what existed in the specimens used to develop Eq. 3.1, this empirical relationship was used to compute "basic" splice lengths from which the other specimen lengths were established. Table 3.1 indicates the values that were used for the variables in equation 3.1.

$$l_d = \frac{(10200 d_b)}{\sqrt{f'_c} [1 + 2.5(c/d_b) + K_r] \phi} \quad (3.1)$$

Table 3.1 Variables Used in Eq. 3.1

Rebar Size	f'_c (psi)	d_b (in)	c/d_b (in/in)	K_r *
# 6	6250	0.75	2.00	2.5
# 10	6250	1.27	1.18	2.5

* indicates maximum value allowed in Eqn. 3.1 for confinement.

The three lap-splice lengths used for each bar size were as follows :

Rebar Size	Lap-Splice Length
# 10	1.) 41" (1.3 l_d - Factor provided by ACI 318-89 for ltwt. concrete)
	2.) 32" (l_d)
	3.) 24" (0.75 l_d)
# 6	1.) 19" (1.3 l_d - Factor provided by ACI 318-89 for ltwt. concrete)
	2.) 15" (l_d)
	3.) 12" (0.75 l_d - 12" minimum was used)

(Lap length were rounded to the nearest whole inch)

3.3.3 Confinement (Duct Size / Wall Thickness). The lap-splice confinement was provided by standard structural steel pipe. Steel pipe was chosen because it is readily available and is inexpensive compared with commercial splice devices. In addition, the standard pipe provides more than enough wall thickness to provide adequate confinement. Current corrugated steel ducts may not have adequate wall thicknesses to provide the confinement needed in splicing bars. Furthermore, a greater selection of steel pipe sizes were available than exist for corrugated duct.

Pipe diameter was selected based on two criteria : (1) the width of the lap-splice bars ($2d_b$) had to fit inside the pipe, and (2) the area of the lap-spliced bars should not exceed 50% of the inside area of the pipe. The latter criterion was adopted from grouted recommendations for tendons published in the Post-Tensioning Manual [15]. Final duct sizes and quantities are listed in Table 3.2. Note that for this particular application, the two criteria yield the same required pipe size. The wall thickness for the pipes chosen were as follows :

1-1/2" Nominal Standard Pipe	0.145 in.
3" Nominal Standard Pipe	0.216 in.

Table 3.2 Determination of Required Duct Size

Rebar Size	d_b (in)	A_b (in ²)	Min. Area based on $2d_b$ (in ²)	$4A_b$ (in ²)	Nominal Pipe Diameter (in)	Duct Area Provided (in ²)
# 6	0.75	0.44	1.77	1.76	1.5	2.04
# 10	1.27	1.27	5.07	5.08	3.0	7.39

3.3.4 Non-Shrink Grout Strength. The non-shrink grout utilized in the study was a mid-range strength grout manufactured by COREMIX with the trade name Supreme Plus. This particular premixed non-shrink grout was chosen based on its rated compressive strength and history of use in post-tensioning applications. The grout strength and grouting procedure are described later in Section 3.5.2.

3.3.5 Concrete. A concrete mix design of 4000psi minimum required compressive strength was selected because it was anticipated that the steel pipe would dominate the behavior of the splice. Higher strength concrete may have enhanced the stiffness of the pipe surrounding the splice by some nominal amount.

3.3.6 Loading. A monotonic loading was applied to the lap-splice connection to establish its performance in tension. Future tests may include cyclic loading to further evaluate the suitability of this type of connection for use in seismic applications.

3.4 SPECIMEN DESIGNATION

Each specimen has been identified as shown in Figure 3.2 using the following symbols :
1.) a number identifying the bar size tested in the lap-splice, and 2.) a number (in inches) referring to the splice length.

<u>Rebar Size</u>	<u>Splice Length (in)</u>	<u>Specimen Designation</u>
10	41	1041
	32	1032
	24	1024
6	19	619
	15	615
	12	612

Figure 3.2 Test Designation Key

3.5 MATERIALS

3.5.1 Concrete. A single casting application was performed to create the basic concrete blocks for the six specimens. Mix proportions and average cylinders strengths at three dates are given in Tables 3.3 and 3.4.

Table 3.3 Concrete Mix Design Proportions

Components	Mix Quantities (pounds per cubic yard) (09/24/93)
Cement	1390
Coarse Aggregate (3/8")	4880
Fine Aggregate (sand)	5340
Water	530
Pozz. R.	61

Table 3.4 Concrete Mix Design Compressive Strengths

Day of Cylinder Test	Compressive Strength (psi)
7-day Strength	4000
14-day Strength	4290
28-day Strength	4740
Strength @ Testing	4860

3.5.2 Non-Shrink Grout. The grout used in the confined lap-splice duct was a premixed non-shrink grout manufactured by COREMIX with the trade name Supreme Plus meeting the specifications of ASTM C1107. A total of fifteen 2"x2"x2" grout cubes were cast during the grouting process to determine the compressive strength of the grout both at 28 days and at the time of testing. Grouting of the specimens was accomplished using two mixes. One mix, from which nine test cubes were cast, was used in grouting the #6 bar splices. A second mix, from which six test cubes were cast, was used in the #10 bar splices.

Grout compressive strength at 28 days and at the time of testing for specimen 612 is shown in Table 3.5, and was computed as the arithmetic average of three 2"x2"x2" test cubes. Grout was poured into one end of each specimen while a thin rod was used to consolidate the material. Bar alignment was maintained throughout the casting and curing procedure. It is anticipated that grout ports would be used in actual precast construction to grout the connection.

Table 3.5 Non-Shrink Grout Compressive Strengths

Test Identification	Grout Strength 28 day (psi)	Grout Strength 42 day (psi)	Age of Grout at Testing (days)
612	7250	8180	42
615	7250	8180	57
619	7250	8180	60
1024	6110	6490	62
1032	6110	6490	64
1041	6110	6490	67

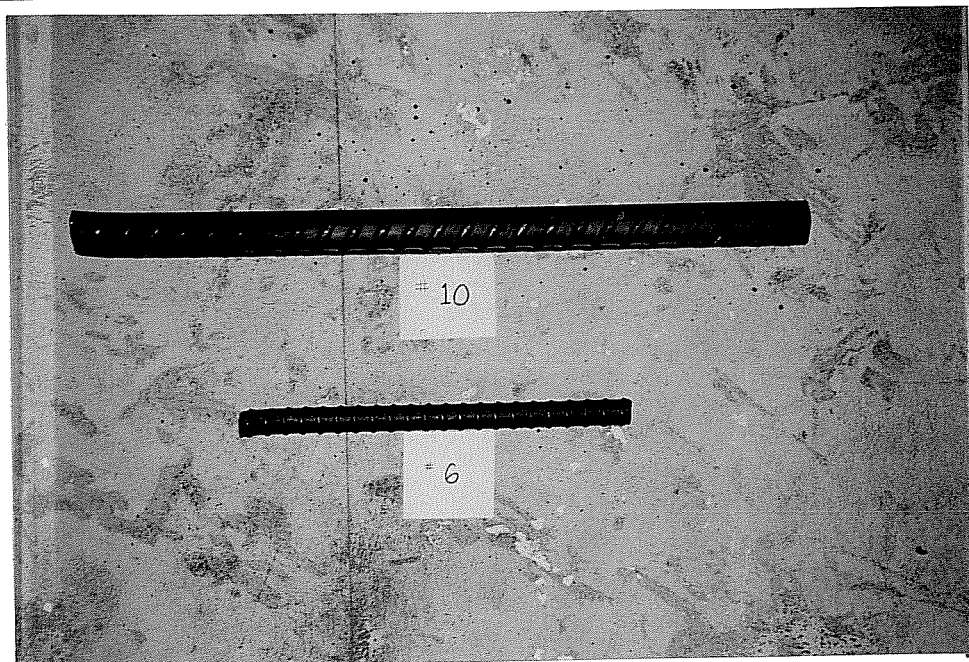


Figure 3.3 Reinforcing Bar Deformation Patterns

3.5.3 Reinforcement. Two Reinforcing bar sizes were utilized in the lap-splice specimens. Both the #6 rebar and #10 rebar were specified with a nominal yield stress of 60ksi. The bar deformation pattern of both rebars is illustrated in Figure 3.3. An 18" long sample of each rebar was used as a tensile coupon. The stress-strain curve obtained for each rebar (#6 and #10) is shown in Figure 3.4. Yield and ultimate occurred at 63.7 and 101.4 ksi for the #6 bar and 65 and 103 ksi for the #10 bar.

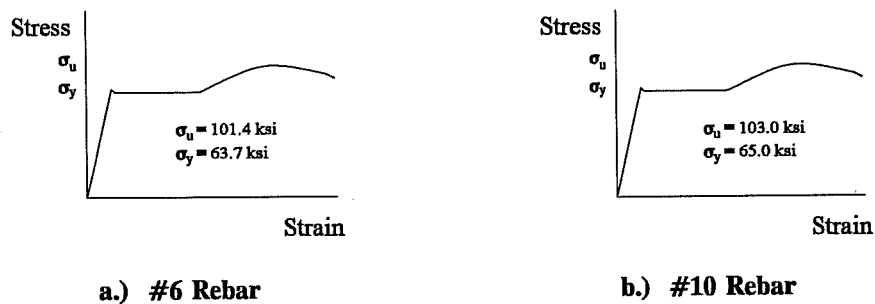


Figure 3.4 Rebar Yield and Ultimate Stresses

3.6 CONSTRUCTION OF THE SPECIMENS

3.6.1 Specimen Construction. Specimen cross sections measured 8-7/8" x 10" for the specimens with #6 rebars and 11-1/2" x 10" for specimens with #10 rebars. Rather than casting a full size column or beam member, specimens were detailed as a single bar test with minimum code cover on one face as would be the case in a column face bar or beam bar. Specimen reinforcement details are illustrated in Figure 3.5.

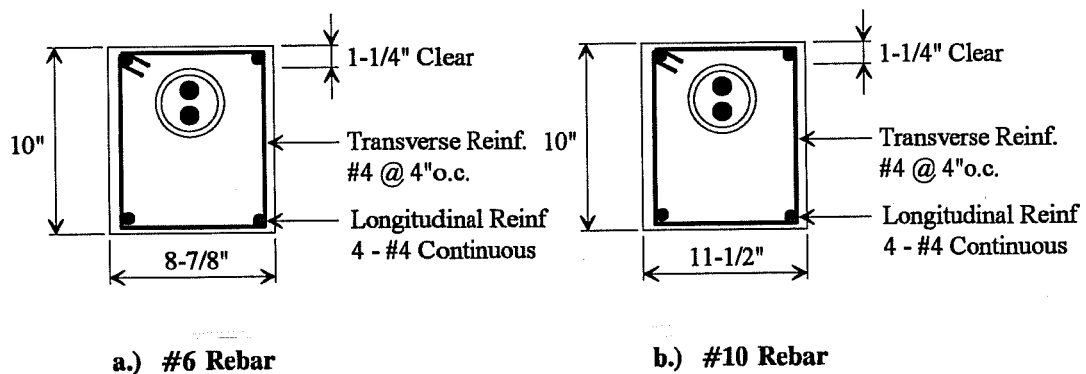


Figure 3.5 Specimen Dimensions and Reinforcement

Forms were constructed with 3/4" form plywood, 2x4's, and 2x6's. Forms were held together with lag screws and 3/8" threaded bolts. Lifting inserts were embedded at both ends and on top in each specimen to facilitate handling and installation of the specimens into the test frame (see Figure 3.6). Forms were oiled prior to placement of steel reinforcing cages and steel ducts.

3.6.2 Longitudinal and Transverse Reinforcement. Specimen reinforcing details for longitudinal and transverse steel were based on Chapter 21 of the ACI 318-89 Building Code [1] for reinforced concrete requirements in seismic locations. Figure 3.5 details the typical transverse and longitudinal reinforcement based on ACI. Complete formwork is shown in Figure 3.7.

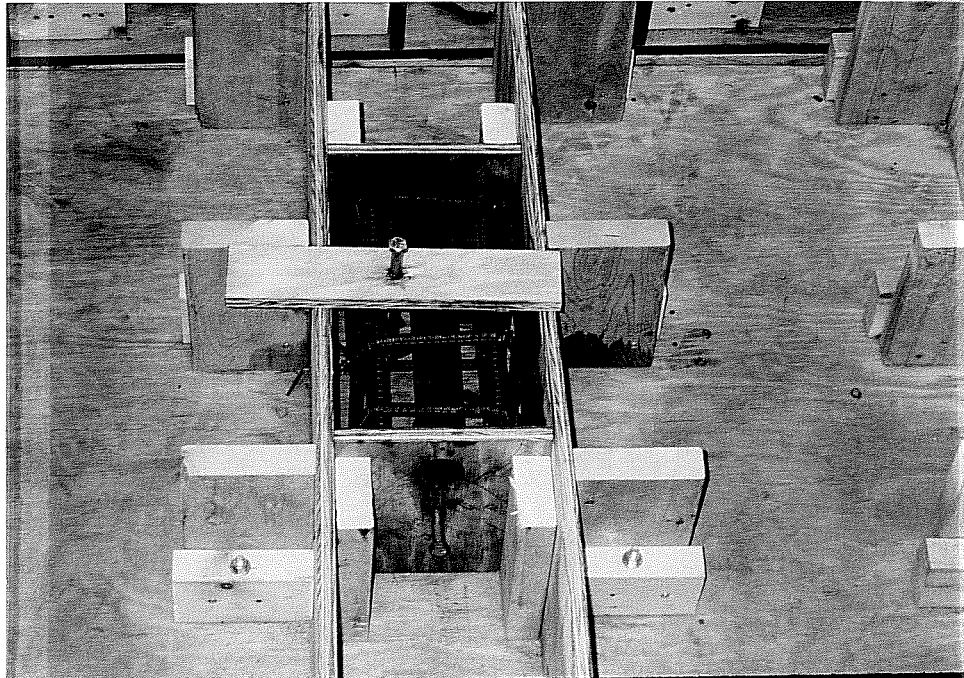


Figure 3.6 Completed Formwork with Inserts

3.6.3 Casting of Specimens. The six specimens were cast on Sept. 24, 1993. Specimen concrete was placed in the formwork both by hand (see Figure 3.9) and with the use of an overhead bucket. Concrete was placed and vibrated in specimens in two layers, then specimens were screeded and finished (see Figure 3.8). Finally, wet burlap and plastic was placed over the specimens during curing. After four days, specimens were removed from the formwork and were prepared for grouting.

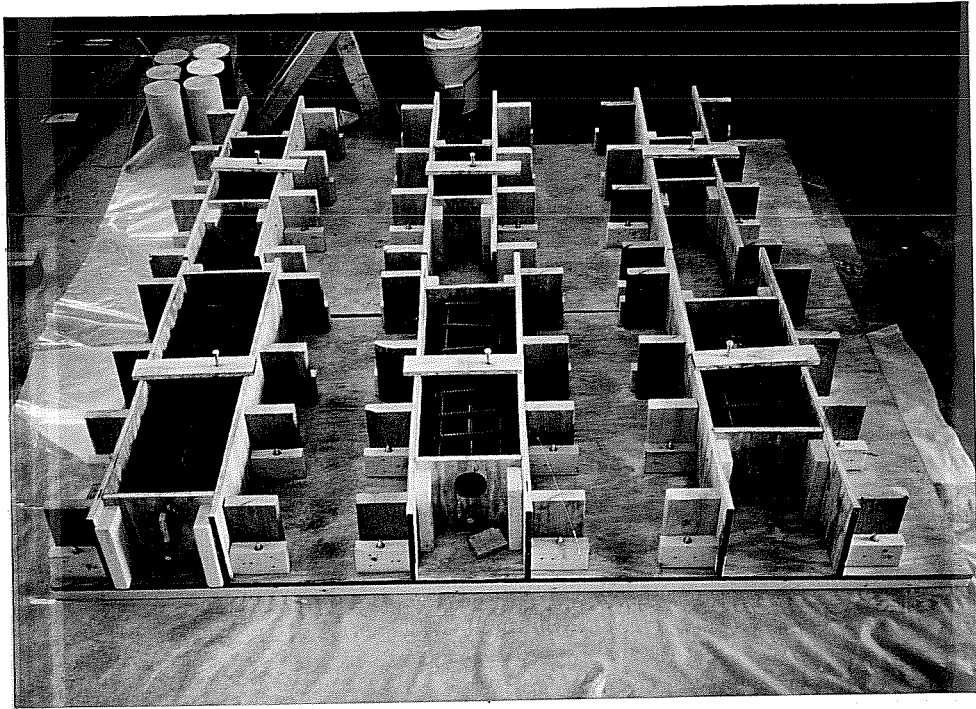


Figure 3.7 Completed Formwork



Figure 3.8 Completed Casting of Specimens



Figure 3.9 Placement of Concrete in Formwork

3.6.4 Non-Shrink Grout Application. Non-shrink grout was prepared as recommended by the manufacturer. Two separate mixes were prepared to grout the six specimens.



Figure 3.10 Grout Mix Set-up

Manufacturer recommendations specified 1-1/4 gallons to 1-1/2 gallons of water per 55 lb bag of grout based on desired flowability. Mix A, which was used to grout the #6 rebar lap splice specimens, was mixed with 1-1/4 gallons of water per 55 lb bag of grout. Mix B contained 1-1/2 gallons of water per 55 lb bag of grout and was used to grout the #10 rebar lap splice specimens. Grout was mixed using a paddle-type mortar mixer (see Figure 3.11). Grout was then poured in the duct while in a flowable state (see Figure 3.12). Prior to grouting, specimens were placed in a vertical position to assure alignment of the rebar, as well as, complete grouting of the duct. In addition, a small bar was used to vertically rod the grout to ensure consolidation of the grout (see Figure 3.13). The non-shrink flowable grout was placed with the specimen in an exterior open-air location. The outdoor ambient temperature varied between 55 degrees F at night to 75 degrees F during the day. Specimens were allowed to cure outside for a minimum of 36 hours then were moved inside the testing laboratory where they were allowed to cure in a horizontal position for a minimum of 28 days before testing.

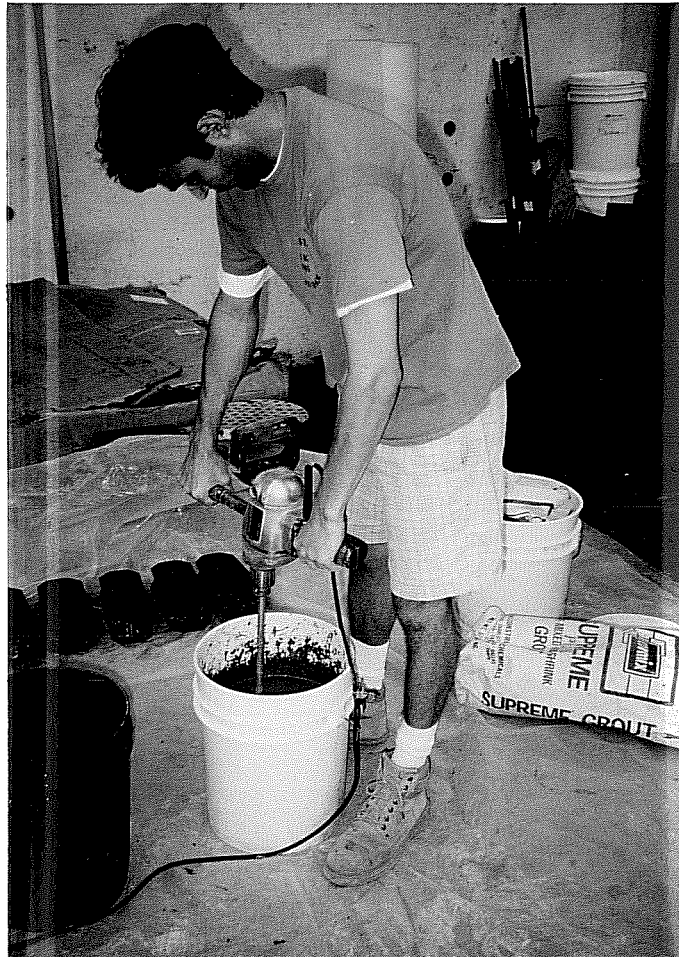


Figure 3.11 Paddle Mixing of Non-Shrink Grout

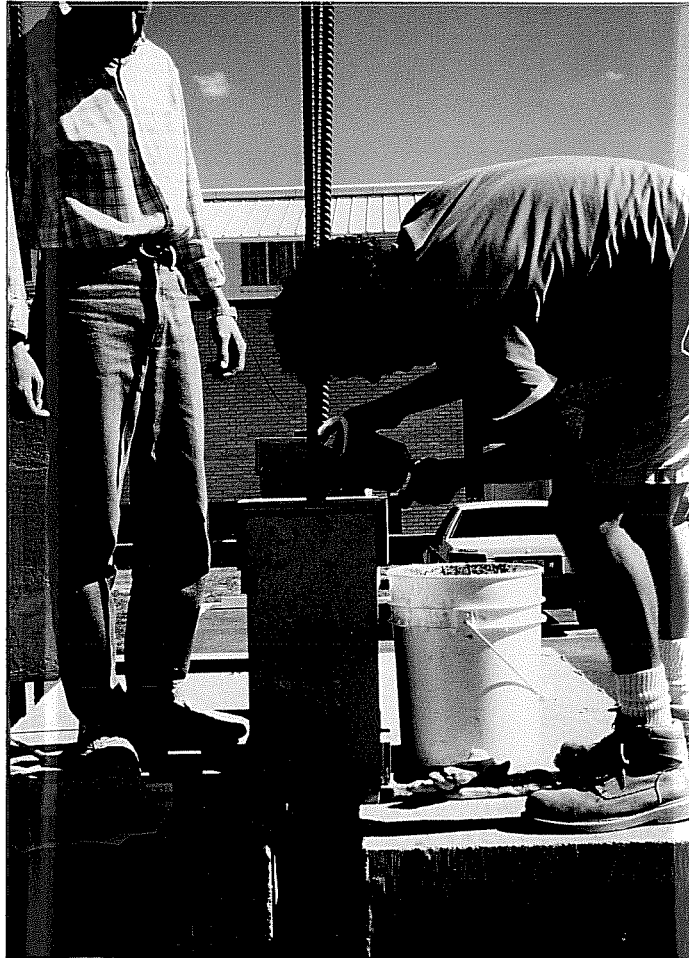


Figure 3.12 Flowable Non-Shrink Grout Placement In Specimen



Figure 3.13 Rodding of Non-Shrink Grout

3.7 TEST FRAME

The test frame illustrated in Figures 3.13 through 3.15 was designed to provide sufficient capacity to ensure loading of the steel element in tension parallel to the interface plane. The frame was fabricated from four W21x57 steel beams with 3/8" stiffeners, four S6x12.5 with cap plates, and 1/2" plates. Four C8x11.5 channels were used to tie the steel frame together. A C6x10.5 channel and two 1" dia. rods were used to vertically restrain the dead end of the specimen. "Dead end" refers to the end of the specimen opposite the end where load is actively applied. The channel and rods coupled with a wooden pedestal under the loaded end of the specimen were used to counteract the tendency of the specimen to rotate which was caused by the eccentricity of the two bars when load was applied. Teflon pads / sheets were placed between the specimen and these restraint locations to allow the concrete block to slide in the direction of loading.

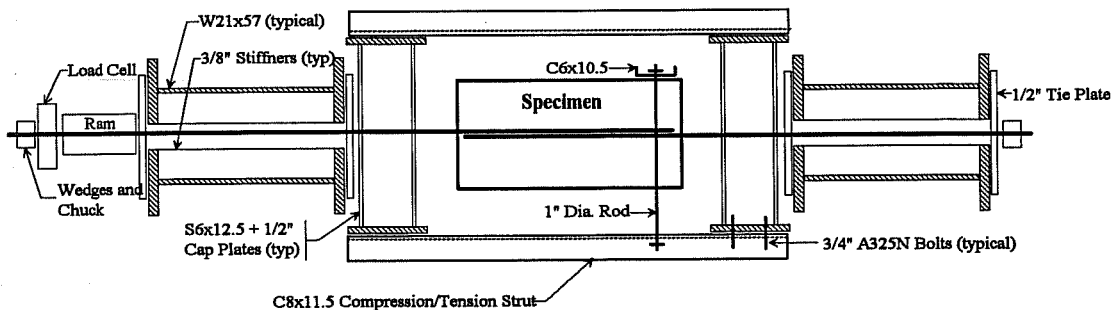


Figure 3.14 Plan View of the Test Frame

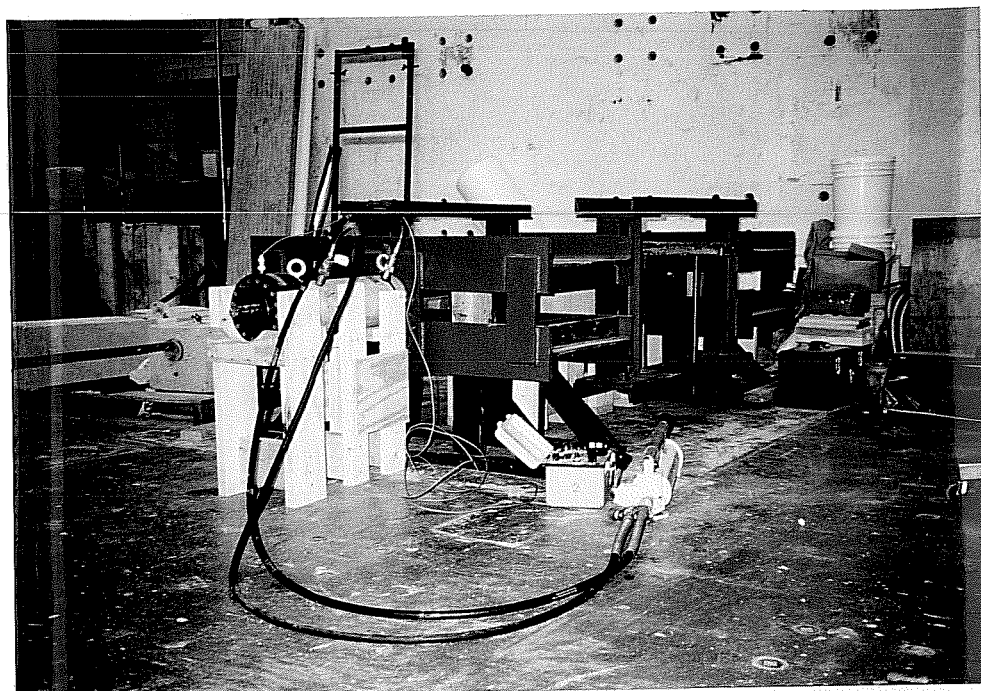


Figure 3.15 Overall View of the Test Set-Up With Specimen



Figure 3.16 Side View of Specimen in Frame

useful in visibly determining any bar slippage. Analytically, bar slip was easily verified once bar deformations were subtracted from the dial gage readings.

3.9 INSTRUMENTATION AND DATA ACQUISITION

3.9.1 Measurement of Displacements. Bar deformations were measured with a dial gage located at each end of the specimen (see Figure 3.18). Dial gages were attached to the rebars and bore against a piece of glass which was attached to the concrete specimen with silicon. The glass provided a consistent surface to measure against on the specimen. Dial gages were accurate to 1/10,000 of an inch.

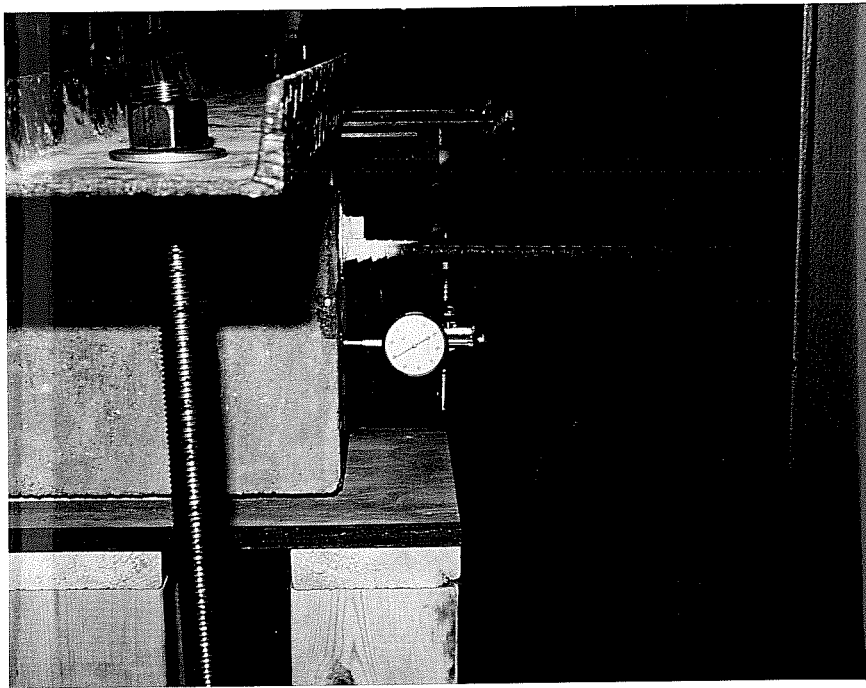


Figure 3.18 Dial Gage Measurement Set-Up

3.9.2 Data Acquisition. The applied load-deformation relationship was continuously monitored using the load cell and dial gages for bar deformations. Load-deformation results were recorded every 1 or 2 kips based on the specimen rebar size. Load-deformation responses were plotted with the use of a spreadsheet program.

CHAPTER 4

PRESENTATION OF EXPERIMENTAL RESULTS

4.1 INTRODUCTION

Results of the confined lap-splice tests are presented in this chapter. Observations from the tests and comparisons between selected responses are presented. Data is presented graphically in the form of load-deformation plots.

4.2 LOAD HISTORY

Specimens were loaded in 1 kip increments for the #6 rebar tests and 2 kip increments for the #10 rebar tests. Loading of the specimens was continued until severe bar slippage occurred or a stress of $1.25 f_y$ (based on actual yield) or greater was reached. Loading was not continued substantially beyond $1.25 f_y$, because the capacity of the steel wedges used to grip the bars was not well known, and because commercial mechanical bar splice devices are only required to develop $1.25 f_y$ (based on nominal yield).

Test progress was monitored using a load cell and strain indicator to determine applied load, and a dial gage at each end of the specimen was used to determine bar deformations (bar slip and bar deformation) relative to the ends of the duct. Some error in bar deformation may have occurred at high loads due to the manner in which the dial gages were attached to the reinforcing bars. The clamps used to attach the dial gages tended to loosen (due to poisson's effect) at high stresses in the bar. This was continuously monitored and clamps were tightened periodically to minimize slip of the gages.

4.3 CONNECTION CAPABILITIES

The maximum load applied to each specimen is listed in Table 4.1, along with the maximum bar deformations measured at the specimen ends. None of the specimens failed as the result of excessive bar slip.

Table 4.1 Summary of Load-Response Data

Test Identification	Maximum Load Applied (kips)	Maximum Bar Deformation (inches)	
		Live End	Dead End
612	37.0	0.222	0.169
615	37.0	0.157	0.141
619	37.0	0.140	0.139
1024	106.0	*	0.379
1032	106.0	0.234	0.245
1041	106.0	0.216	0.209

* - A single deformation reading is shown due to a dial gage malfunction.

4.4 LOAD VERSUS DEFORMATION RESPONSE

Load versus deformation responses for this series of tests are presented in Sections 4.4.1 and 4.4.2. All specimens exhibited a load-deformation response representative of a standard coupon test for rebar tested in air. In other words, it appeared minimal bar slippage occurred during loading. Confinement provided by the duct appeared to significantly decrease the required splice length of the reinforcing bars. This will be illustrated and discussed at greater length in the Chapter 5.

4.4.1 Response of Confined Lap-Splice Specimens with #6 Reinforcing Bars. Three specimens were tested monotonically in tension with lap-splice lengths of 12, 15, and 19 inches.

Tables A.1 through A.3 list the load-deformation response data for each test. The load-deformation response for both the "live end" and "dead end" are presented in Figures 4.1 and 4.2. Measured response of specimen 619 is presented in Figure 4.3 to demonstrate that the behavior of the two ends was comparable.

4.4.1.1 Specimen 612. The 12" lap-splice was tested prior to placement of the steel channel that was added to prevent vertical rotation of the specimen. During testing of the specimen, a slight rotation due to the eccentricity of the spliced bars was noted. It appeared that the rotation did not affect the measured deformation readings as represented in the load-deformation responses (Figures 4.1, and 4.2) at levels of loading below yielding of the reinforcement. However, at loadings above yielding of the reinforcement, the rotation appeared to effect the load-deformation response of the reinforcing at the dead end. Since specimen 612 had the smallest moment arm and rotation was not restricted, the couple forces caused by the bar eccentricities produced a bending or kinking in the exposed dead end rebar between the face of the specimen and the wedges. It was felt this bending restricted bar-slippage at high loads since the exposed rebar was influenced by a vertical couple force. Load-deformation response for this specimen was less stiff than for the other two specimens containing #6 bars, and the behavior was qualitatively comparable to the shortest lap-splice specimen containing #10 bars.

4.4.1.2 Specimen 615. Due to the slight rotation during the testing of specimen 612 a C6 channel section was placed above the dead end of the specimen to restrict any rotation in the vertical plane. In addition, teflon sheets were placed between the channel and specimen and the specimen and base support at the live end to facilitate horizontal movement in the direction of loading (see Figure 4.4) for the testing of all remaining specimens. The testing of specimen 615 was preformed without any noticeable problems or inconsistencies.

Figure 4.1 Load-Deformation Response, #6 Bar Lap-Splice (Live End)

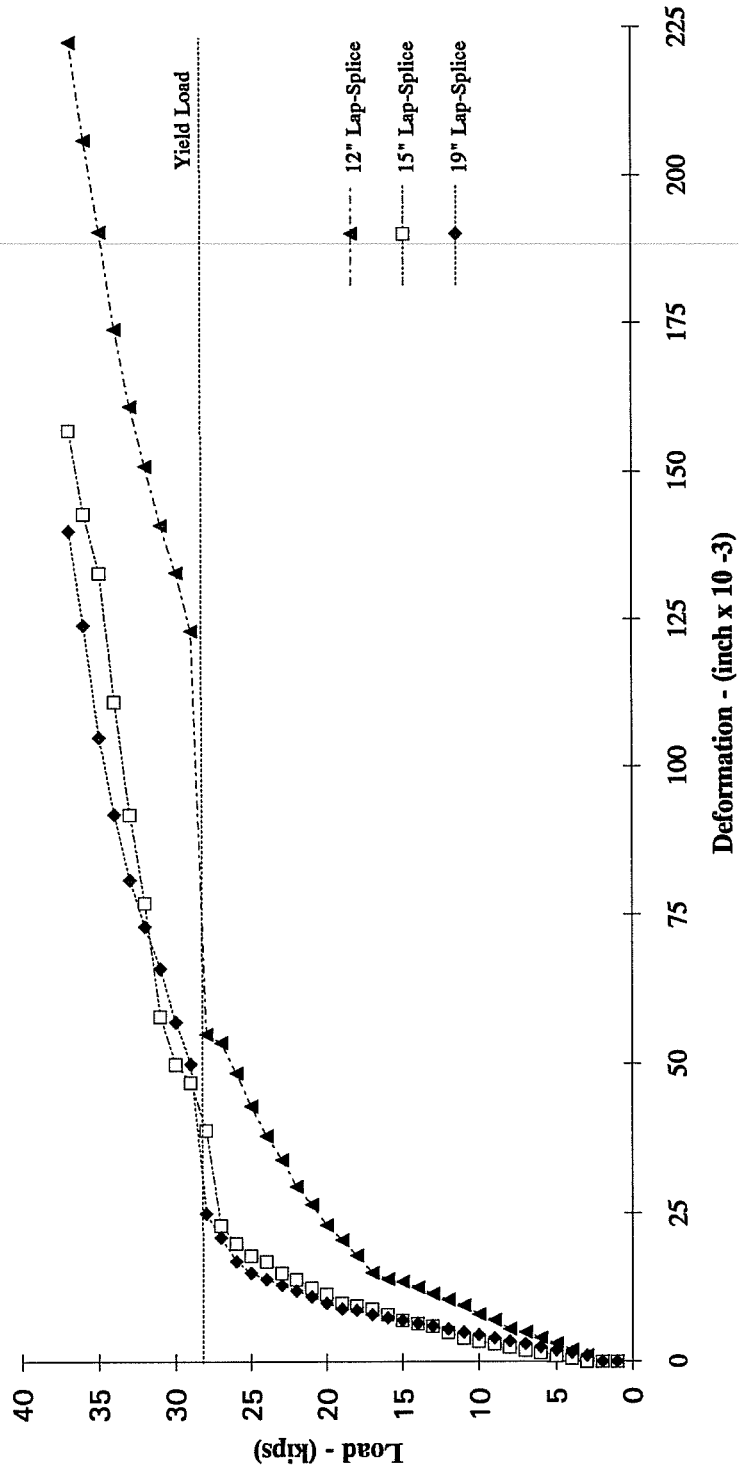


Figure 4.2 Load-Deformation Response, #6 Bar Confined Lap-Splice (Dead End)

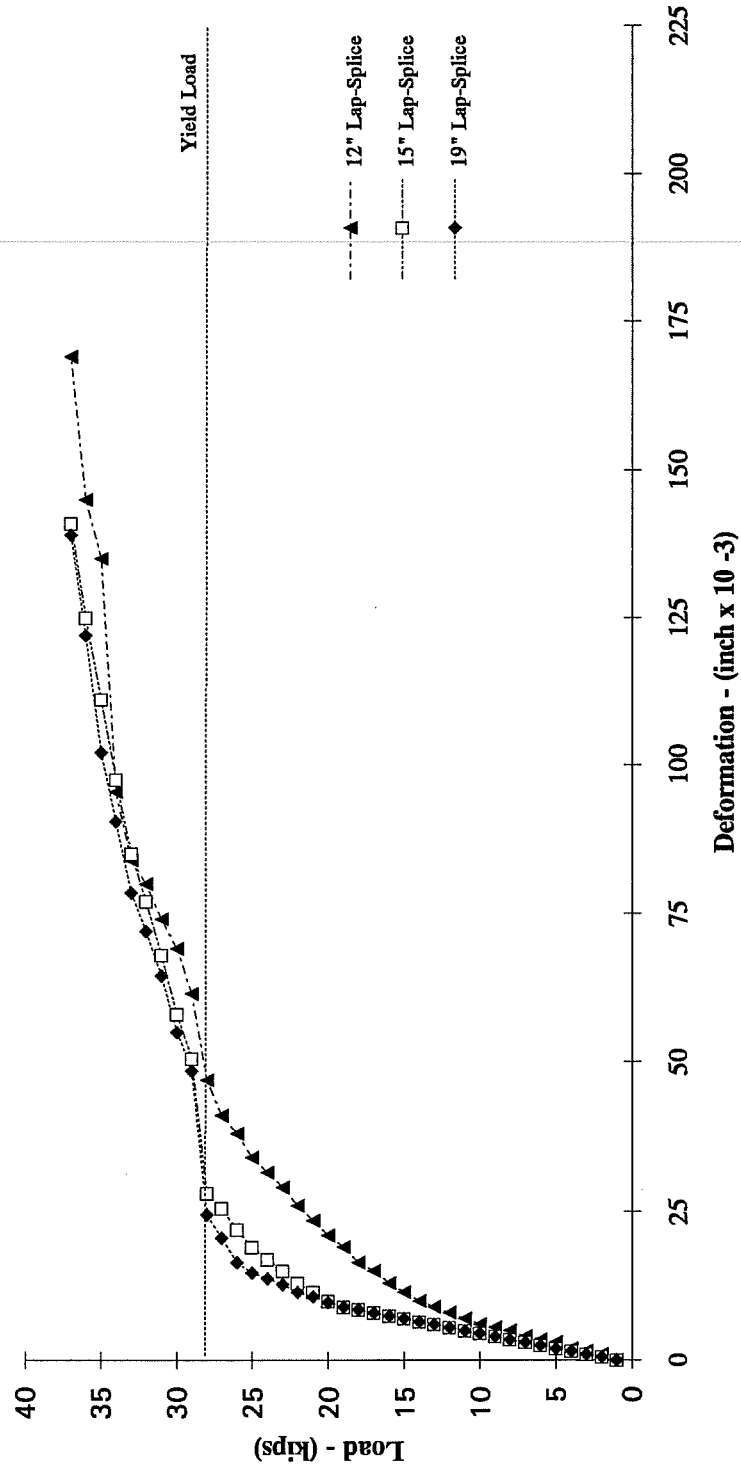
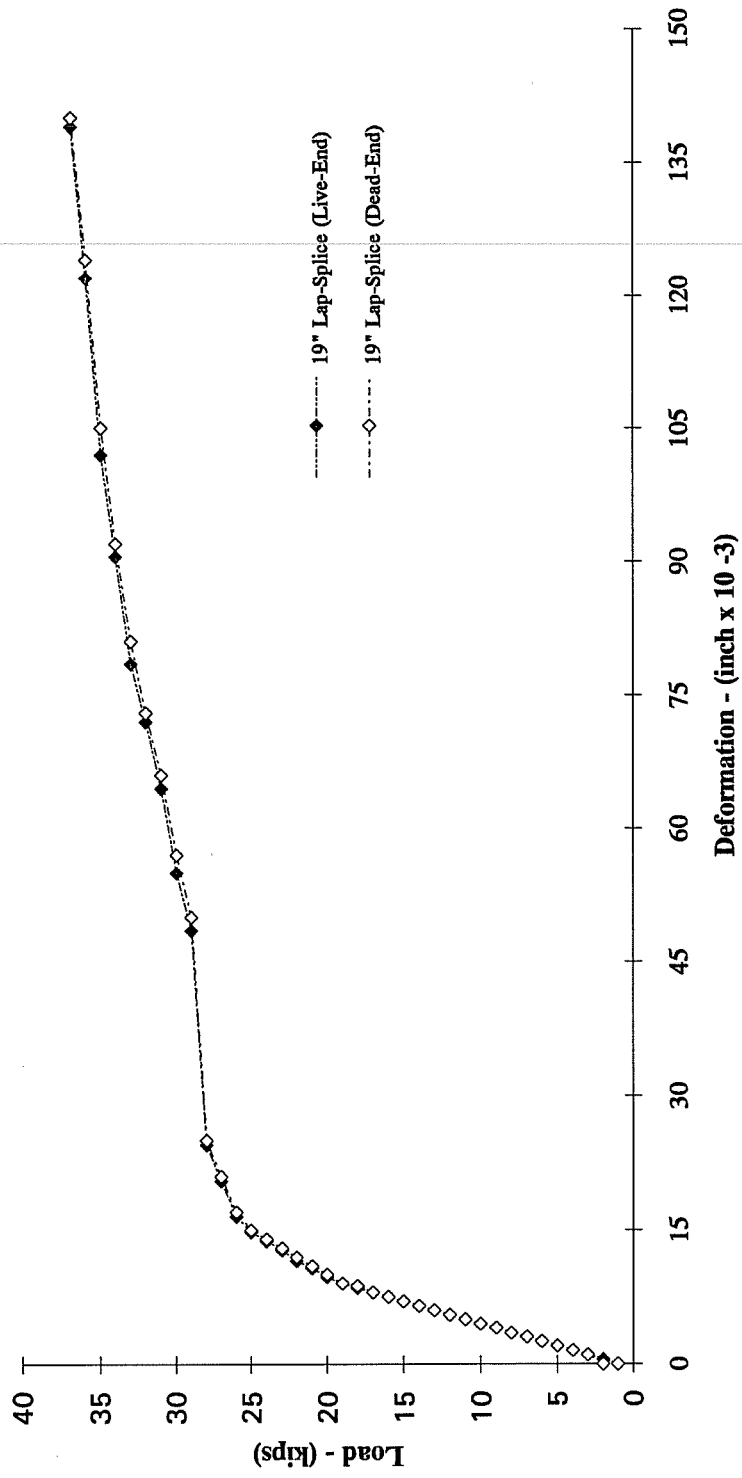


Figure 4.3 Live End and Dead End Response Comparison



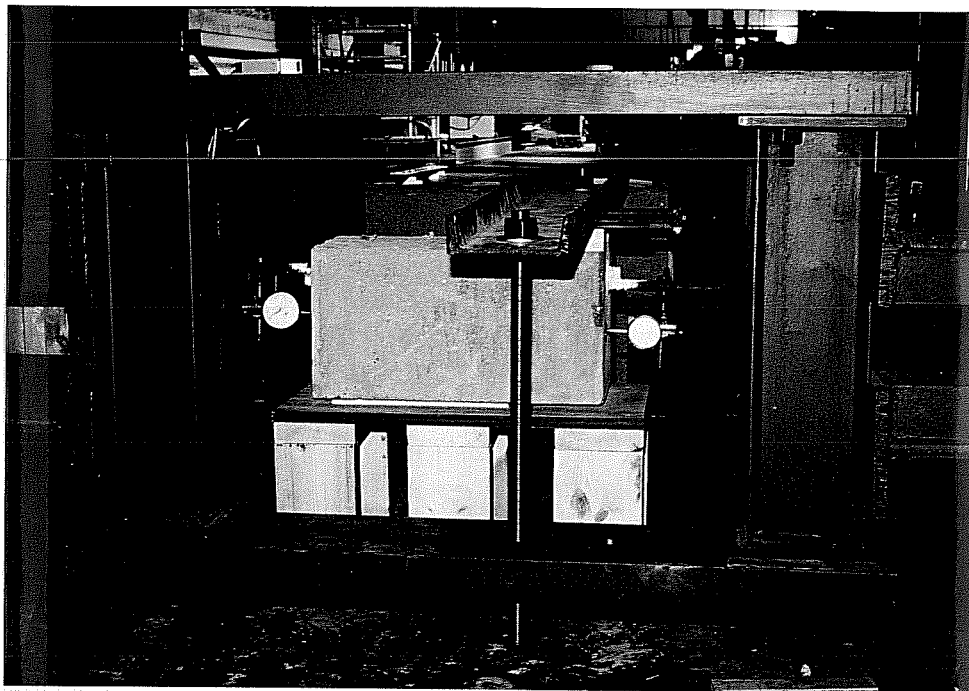


Figure 4.4 Test Frame with Teflon Pads for Unrestrained Horizontal Movement

4.4.2 Response of Confined Lap-Splice Specimens with #10 Bar Reinforcing. Three specimens were tested monotonically in tension with lap lengths of 24, 32, and 41 inches. Tables A.4 through A.6 detail the load-response data of each test. In addition, the load-deformation response of both the live end and dead end are presented in Figures 4.6 and 4.7. A comparison of the load-deformation response is presented in Figure 4.8.

4.4.2.1 Testing of Specimen 1024. Testing of specimen 1024 was performed with one noticeable problem and a subsequent inconsistency. During the test, the dial gage at the live end malfunctioned. For this reason no load-deformation response is presented in Figure 4.8. In addition, the load-deformation response at the dead end appears to be questionable due to the exhibited loss in stiffness followed by an increase in stiffness. Figure 5.3 depicts a modified 24" lap-splice which is believed to be a better representation of the load-deformation response.

Figure 4.6 Load-Deformation Response, #10 Bar Confined Lap-Splice (Live End)

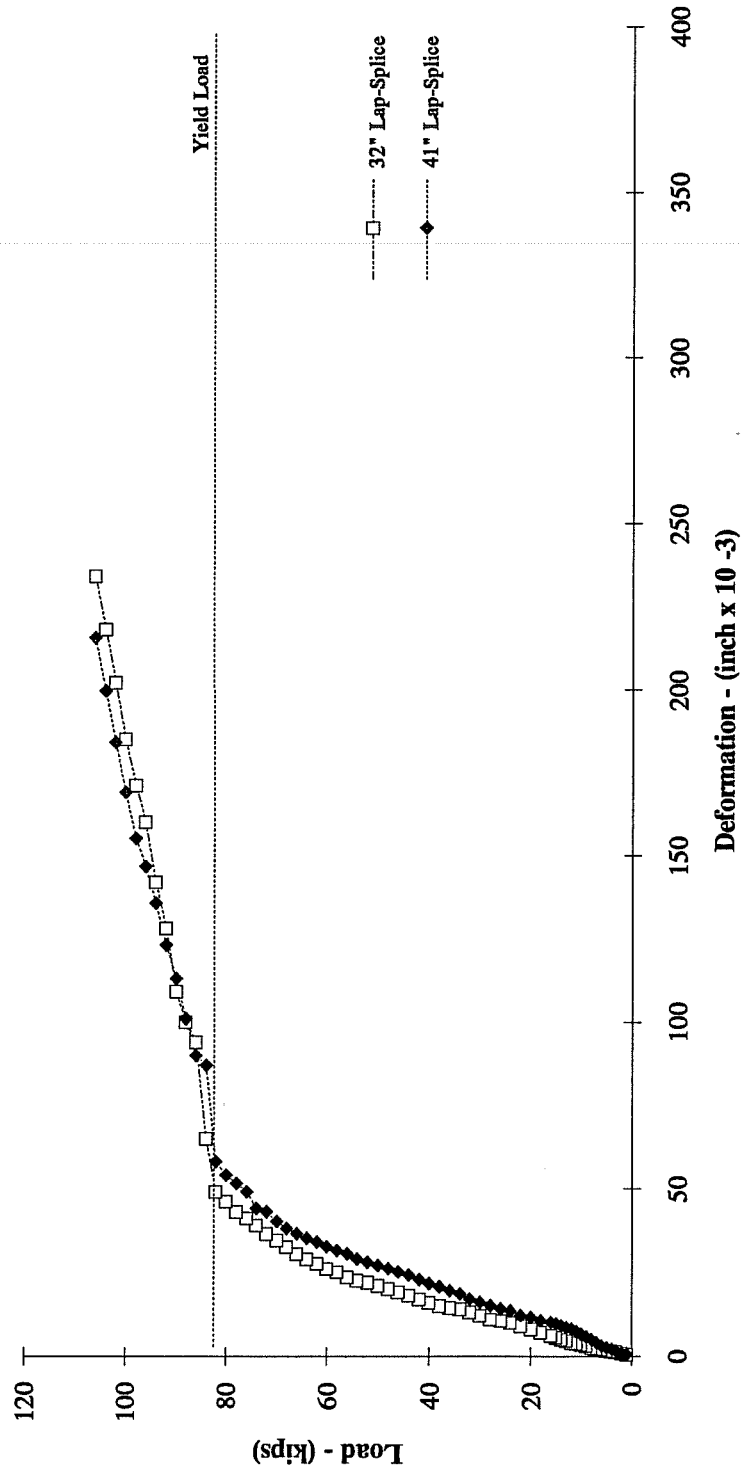


Figure 4.7 Load-Deformation Response, #10 Bar Confined Lap-Splice (Dead End)

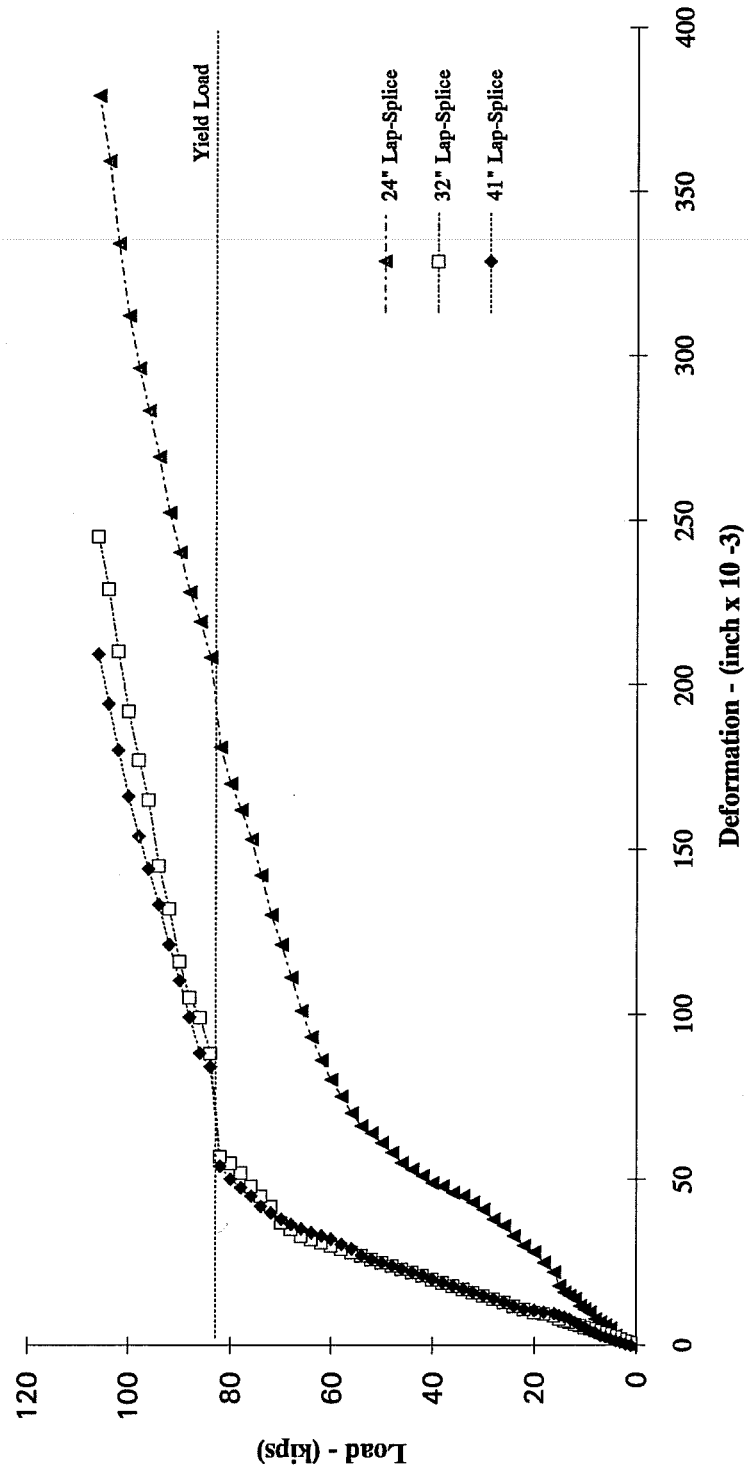
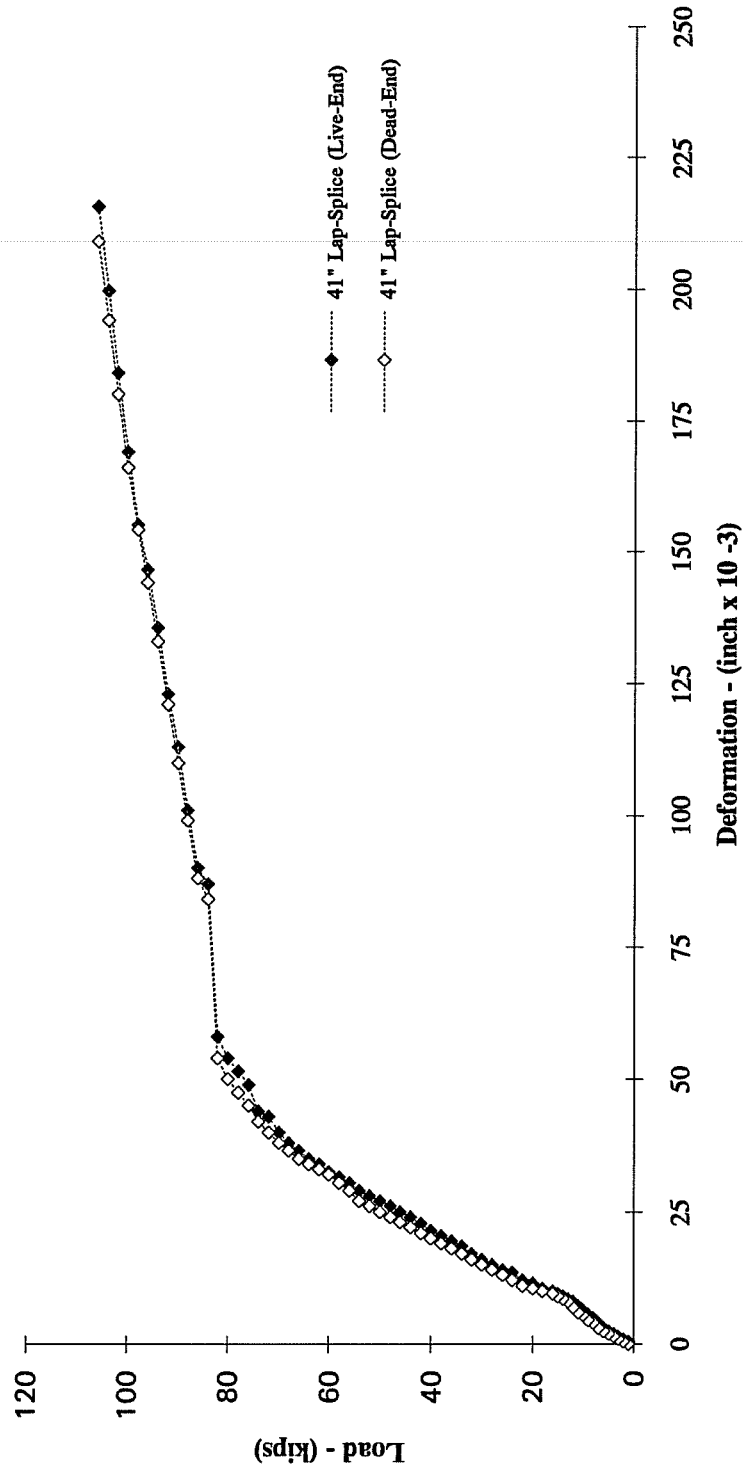


Figure 4.8 Live End and Dead End Response Comparison



CHAPTER 5

EVALUATION OF RESULTS

5.1 INTRODUCTION

Load-deformation response curves obtained in this study are compared and provisions published in the ACI Building Code [1] and by Orangun, Jirsa, and Breen [14] for bar splices in tension are examined in light of the experimental results. In addition, bar deformations at service-level loads in the tests are related to crack widths in members and are compared with recommended crack width limits to judge the performance of the test specimens.

5.2 REFLECTION ON EXISTING SPLICE PROVISIONS

The splice lengths for all test specimens in this study were based on a multiplier less than or equal to unity times a basic development length recommended by Orangun, Jirsa, and Breen. Since the ducts which contained the spliced bars were filled with a cement grout, a 1.3 factor was applied to the basic development length. Furthermore, the strength reduction factor, ϕ , of 0.8 was included to effectively account for a stress level in the steel of $1.25f_y$ instead of f_y . The term which is related to confinement, K_{tr} , was taken as the maximum value suggested by Orangun et al. (2.1). The quantities computed using Equation 5.1 are tabulated in Table 5.1 also included the measured grout compressive strengths (listed in Table 3.5) and included the actual yield strengths of the #6 and #10 bars (63.7 and 65ksi, respectively) by substituting 10,830 and 10,980 for 10,200 in the numerator of Equation 5.1.

$$l_d = \frac{(10200 d_b)}{\sqrt{f'_c} [1 + 2.5(c/d_b) + K_{tr}] \phi} \quad \text{for } f_y = 60 \text{ ksi} \quad (5.1)$$

In addition, splice lengths were computed using the basic development length equation given by ACI 318-89. The basic development length was multiplied by a 1.3 factor (for ltwt. concrete), and the yield strength of the steel was replaced by the actual yield strength from the

coupon tests. The resulting calculated splice lengths for #6 and #10 bars are also included in Table 5.1.

$$l_d = \frac{A_b(1.25f_y)}{\pi d_b(9.5\sqrt{f'_c}/d_b)} = 0.04 A_b f_y / \sqrt{f'_c} \quad (\#11 \text{ and smaller}) \quad (5.2)$$

In Chapter Four it was reported that all six specimens were capable of developing $1.25f_{y(\text{actual})}$, and large deformations which were intended to accompany the $1.25f_y$ stress. The minimum lap-splice lengths used in the tests for both the #6 and #10 bars are listed in Table 5.1. It is interesting (and not surprising) that the computed lap-splice lengths exceeded the minimum lengths which successfully developed $1.25f_{y(\text{actual})}$ by 58 and 97% for the #6 and #10 bars when the lap length computed by the Orangun equation, and by 35 and 122% when the lap was computed using ACI 318-89. Considering the substantial amount of steel that envelopes each splice in this test series, it seems obvious that confinement plays a tremendous role in reducing the lap length required to develop $1.25f_y$. Even though the Orangun equation explicitly considers the effects of confinement, the maximum value for the confinement term, K_{tr} , recommended by Orangun et al. is based on tests with confinement levels that do not approach what was offered by the pipes used in these tests. It is interesting to note that if K_{tr} is computed without limit for the pipes used in these tests, the resulting splice lengths for the #6 and #10 bars (including the 1.3 factor for ltwt. concrete) are 3.3 and 7.4 inches, respectively. The fact that these are substantially shorter than the lengths actually tested suggests that Equation 5.1 is indeed not suited for calculating the lengths of these highly confined lap-splices, and also suggests that further testing with a much

Table 5.1 Comparison of Computed Lap-Splice Lengths with Minimum Test Lengths

Reinforcing Size	Orangun et al. $1.3 l_d$ (inches)	ACI 318-89 $1.3 l_d$ (inches)	Specimen Test Length* (inches)
# 6	19.0	16.2	12.0
# 10	47.2	53.3	24.0

* - Minimum splice length tested.

expanded set of variables should be conducted to develop a splice equation for highly-confined bars.

5.3 COMPARISONS BETWEEN LOAD-DEFORMATION RESPONSES

Before making comparisons between the #6 and #10 bar specimen responses, elastic deformations that occurred between each end of the concrete, block, and the point where the dial gage was mounted on the reinforcing bar were subtracted from the measured response. The modified load-deformation responses (average between live and dead ends) up to yield are presented in Figures 5.2 and 5.3. Comparisons between the elastic stiffness of load-deformation responses indicates that two of the three #6 lap-splice specimens had a higher stiffness than the companion #10 specimens.

There are three possible reasons that specimen stiffnesses would be higher for the #6 specimens: grout compressive strength, bar surface area to volume ratios, and lug layout and spacing. Grout Mix A which was used in the #6 rebar specimens had a reduced water / mix proportion ratio compared with Mix B and yielded a higher compressive strength of 8180 psi versus 6480 psi for Mix B. Assuming the bond strength to be a function of $\sqrt{f'_c}$, and all other factors to be equal, the compressive strength difference would require approximately a 12% increase in the development length for the #10 rebar specimens. Although these strength differences agree with the trends noted above, a 12% variation would likely be lost in the scatter associated with this type of test data.

The #6 rebar specimens have a greater surface area-to-volume ratio than the #10 rebar specimens (5.33L vs. 3.15L). As a result, the #6 rebar specimens can develop a given level of bar stress while experiencing lower average bond stresses than will be experienced by the #10 bars. In both analytical and laboratory research performed at the University of California at Berkeley [9], a 21% increase in maximum bond resistance was observed when bar size was decreased from a #10 to #6.

Pattern and spacing of lugs on deformed rebars influences bond characteristics [9]. As displayed in Figure 3.3, the lug pattern and spacing for the #10 bar was a crescent pattern spaced on center at 13/16 in. compared to a horizontal lug pattern at 1/2 in. spacing for the #6 bar. The influence of the deformation pattern can best be described by the so called "related rib area", α_{rR}

[9], which is the ratio of the bearing area (area of the lugs perpendicular to the bar axis) to the shearing area (perimeter times lug spacing).

$$\alpha_{sR} = \frac{k F_r \sin \beta}{\pi d_b c} \quad (5.3)$$

where :

k	=	number of transverse lugs around perimeter
F_r	=	area of one transverse lug
$\sin \beta$	=	angle between lug and longitudinal axis of bar
c	=	center-to-center spacing between transverse lugs

It should be noted from Equation 5.3 that increased spacing between lugs and reduction in the angle between the lug and longitudinal axis of the bar reduces the "related rib area" and thus bond strength. Therefore Equation 5.3 applied to the lug pattern and spacing for the bars used in this study indicate better bond behavior for the #6 bar than for the #10 bar. As an additional note, reinforcing bars used in the United States have α_{sR} values ranging from 0.05 to 0.08. The α_{sR} values for the #6 and #10 bars were 0.073 and 0.056.

5.4 SERVICEABILITY CONCERNS

Although all six specimens tested were able to develop more than 1.25 times the actual yield strength of the bars, this type of connection will not be acceptable if "large" cracks develop at either end of the lap-splice connection. In order to assess the serviceability of the six connections tested, an allowable crack width at a level of bar stress associated with service-level loads was needed. The discussion which follows identifies and rationalizes such a limit. Gerglely and Lutz suggested an allowable maximum crack widths as noted in Table 5.2. The ACI 318-89 provisions for crack control are based on research conducted at Cornell University which involved statistical analysis of a large amount of crack-width data [18]. Gerglely and Lutz proposed Equation 5.4 for predicting the maximum width of crack at the tension face of a beam.

Table 5.2 Recommended Tolerable Crack Widths For Reinforced Concrete

Exposure Condition	Tolerable Crack Width	
	(inches)	(mm)
Dry Air or Protective Membrane	0.016	0.41
Humidity, Moist Air, Soil	0.012	0.30
Deicing Chemicals	0.007	0.18
Seawater and Seawater Spray	0.006	0.15
Water-Retaining Structures	0.004	0.10

$$w = 0.076 \beta f_s \sqrt[3]{d_c A} \quad (5.4)$$

where : w = max. width of crack (thousands of an inch)
 f_s = steel stress at service load or $0.60f_y$ (ksi)
 d_c = thickness of concrete cover measured from tension face to center of bar closest to that face (inches)
 β = ratio of distances from tension face and from steel centroid to neutral axis, equal to h_2 / h_1
 A = concrete area surrounding one bar, equal to the total effective tension area of concrete surrounding reinforcement and having same centroid, divided by the number of bars (in²)

Current provisions in ACI 318-89 utilize a $\beta = 1.2$ to simplify and reformat Equation 5.4 into Equation 5.5. In this form, allowable crack widths, w , are now represented by the parameter z .

$$z = f_s \sqrt[3]{d_c A} = \frac{w}{0.091} \quad (5.5)$$

Control of maximum crack width is done by proportioning longitudinal reinforcement so that the parameter z is kept below 175 for interior exposure and 145 for exterior exposure. These limits correspond with maximum crack widths of 0.016 and 0.013in., respectively.

While these limits have been developed for flexural members, a correlation with reinforcing bars in direct tension may be drawn from research performed at the University of California at Berkeley during the mid 1980's. The work performed by Eligehausen [9], studied

bond-slip behavior of individual bars under monotonic and cycled loadings. Under monotonic loading the results indicated that the crack width formed by the lugs most nearly equaled the bar-slip up to the point where shear cracks formed following crushing of the concrete. This is illustrated in Figure 5.1.

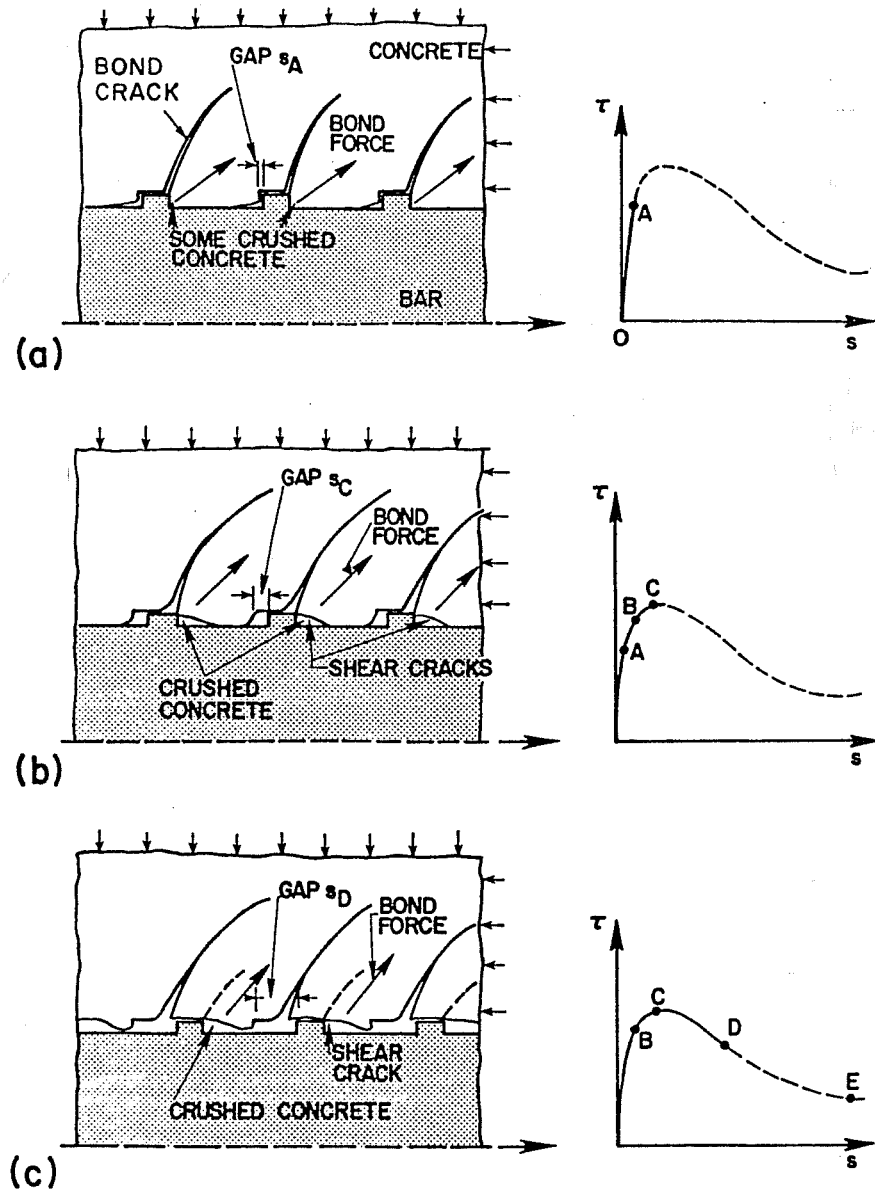


Figure 5.1 Mechanism of Bond Resistance Under Monotonic Loading [9]

It should be noted that the load-deformation responses (Figures 5.2 and 5.3) were similar to the bar-slip responses reported by Elgehausen, with the exception that the resistance of the confined lap-splice responses did not drop off, as a result of the substantial confinement provided.

In order to be consistent with crack width serviceability provisions currently in ACI Building Code, specimen deformations (bar-slip) at a bar stress equal to $0.6f_{y(\text{actual})}$ were compared with an allowable crack width of 0.016 inches. Both of these limits are shown on the modified load-deformation responses presented in Figures 5.2 and 5.3.

5.4.1 Serviceability of #6 Reinforcing Bar Splices. Examination of the modified load-deformation responses for the #6 lap-splice specimens indicates that all three specimens deformed less than the 0.016in. limit at a load corresponding with a stress of $0.60f_y$. However, it is quite clear that the behavior of the specimens with 15 and 19in. lap-lengths was far superior to that measured for the 12in. lap-length. Deformation of the 12in. specimen was approximately three times the deformation of the 15in. specimen. Behavior of the 15 and 19in. lap lengths was nearly identical up to the load corresponding with 60% of yield.

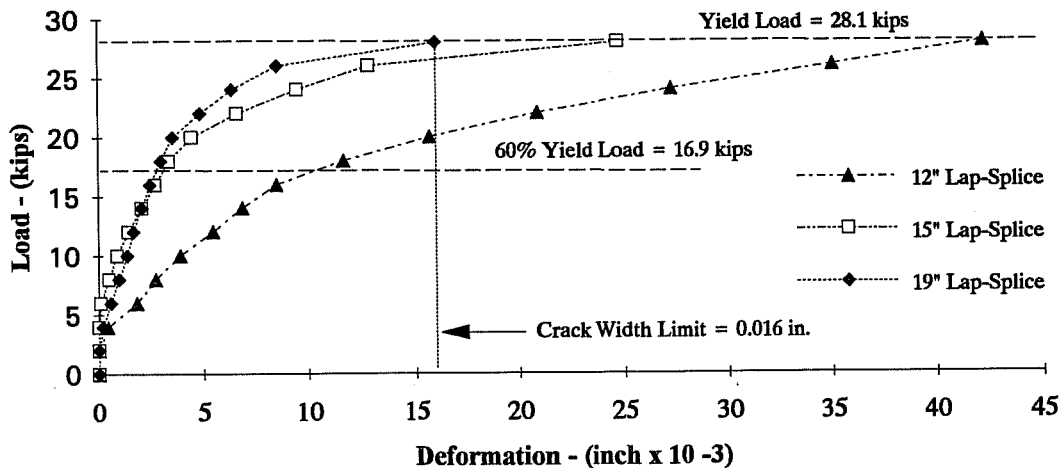


Figure 5.2 Modified Load-Deformation Response, #6 Rebar

5.4.2 Serviceability of #10 Reinforcing Bar Splices. Examination of the modified load-deformation responses for the #10 lap-splice specimens indicates that only the 32 and 41in. specimens exhibited deformations (bar-slip) less than the 0.016in. limit at 60% of the yield load.

The deformation (actual) for the 24in. lap-splice exceeded the allowable deformation by nearly a factor of three.

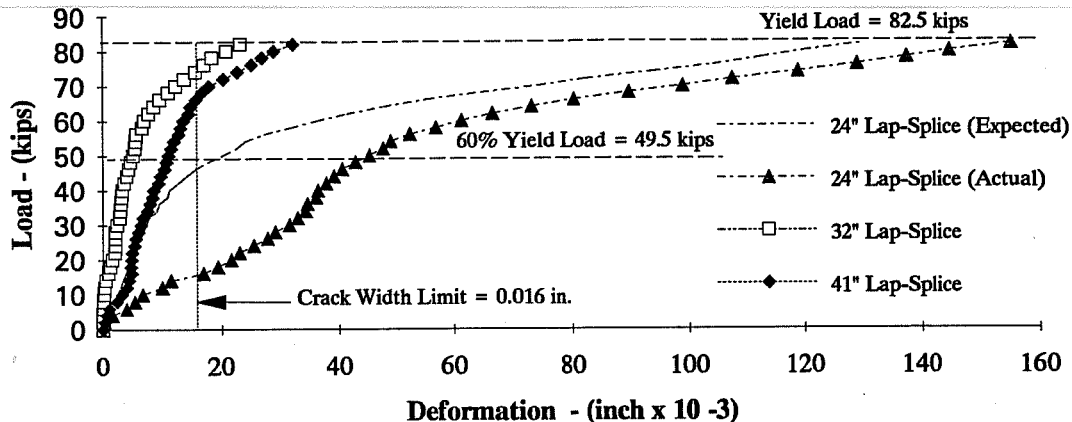


Figure 5.3 Modified Load-Deformation Response, #10 Rebar

Table 5.3 Summary of Connection Evaluation

Lap-Splice Length (inch)	Evaluation for Monotonic Loading
12" Lap-Splice - #6 Rebar	Yes
15" Lap-Splice - #6 Rebar	Yes
19" Lap-Splice - #6 Rebar	Yes
24" Lap-Splice - #10 Rebar	No*
32" Lap-Splice - #10 Rebar	Yes
41" Lap-Splice - #10 Rebar	Yes

Bold letters indicates shortest acceptable lap-splice tested which meets the strength and serviceability criteria presented in this thesis.

* - Lap-splice load-deformation response questionable. The lap-splice may meet the strength and serviceability criteria presented in this thesis.

5.5 DESIGN AND RESEARCH IMPLICATIONS

Confinement in the form of a standard steel pipe significantly improved not only the strength characteristics of the lap-splice connection, but also the "elastic stiffness" and apparent toughness of the lap-splices tested. From a design standpoint, the current ACI 318-89 Building Code provisions and design recommendations by Orangun et al. overestimate the required lap-splice lengths by a minimum value of 35 and 58%, respectively. In order to develop an accurate understanding of how much confinement (diameter and wall thickness), rebar size, and grout strength affect connection behavior, a much more exhaustive testing program must be performed. The research documented in this paper details two very specific confinement and rebar size examples. The very limited test program does indicate that steel pipes, or perhaps a thin-wall duct, can be used effectively to splice longitudinal reinforcement in precast elements.

CHAPTER 6 SUMMARY AND CONCLUSIONS

6.1 SUMMARY

A modest experimental program was implemented to evaluate the feasibility of a grouted lap-splice connection confined by a steel pipe. It was hypothesized that the confinement provided by the pipe would substantially shorten the lap length necessary to develop $1.25f_y$ in the bars. The long-term objective of this investigation and further work that should follow is to develop provisions for a confined lap-splice connection that will provide much more economical connections for use in the precast industry compared with some of the more expensive grouted and mechanical connections now in use.

The series of six tests was composed of three splice specimens containing #6 bars and three specimens containing #10 bars. Pipes used to confine the splices were not varied in each group of three specimens, and grout strengths in the splice connections were intended to be the same. The only variable considered in each group of specimens was the length of the lap-splice. For each group, the lap lengths were based on a fraction of the required splice length computed using empirical provisions developed by Orangun, Jirsa, and Breen [14]. The confined lap-splices, which were embedded in concrete blocks, were tested monotonically in tension. Behavior of the specimens was judged largely from load-deformation (slip) responses measured at each end (the applied load and anchored end) of the specimens. Specimen strengths and stiffnesses were compared, and serviceability of the splice connections was also developed.

6.2 CONCLUSIONS

From the results of this experimental study, the following observations were made for the confined lap-splice connections:

- 1.) All specimens developed more than $1.25f_{y(\text{actual})}$ in the bars, and resistance continued to increase up to the point when each test was terminated. None of the specimens failed during testing.

2.) The steel pipe used to confine the lap-splice connections apparently reduced the lap length required to develop $1.25f_y$ tension in the bars because all specimens were shorter than the lap length computed using Orangun's equation or current ACI 318-89 provisions (and all developed more than $1.25f_y$).

3.) Load-deformation plots for the tests indicated that the #6 bar splices were generally stiffer in the "elastic" range than the #10 bar connections. This was believed to be due to a higher f'_c , a higher surface area-to-volume ratio for the #6 bars, and a closer rib spacing and more favorable rib orientation also for the #6 bars.

4.) A deformation limit of 0.016in. at a stress of $0.6f_y$, based on research conducted by Gergeley and Lutz [18], was imposed on the specimens to effectively limit the crack width that would most likely form at the end(s) of the splice (and pipe). All but the shortest #10 bar splice satisfied this serviceability requirement. However, even though the shortest (12in.) #6 splice satisfied this check, the additional three inches used in the next longest (15in.) #6 splice reduced bar deformations by 32 percent.

5.) Load-deformation (bar-slip) responses for the two specimens in each group that exhibited the best behavior were nearly linear up to yield.

6.3 FURTHER RESEARCH NEEDS

The following is a recommended list of further research needs :

- 1.) Shorter splice lengths should be investigated. (Each specimen tested in this program attained more than $1.25f_y$ without failing.)
- 2.) Wall thickness of the confining duct should be reduced. Perhaps a post-tensioning duct which is substantially lighter and less expensive could be used.

- 3.) Grout compressive strength should be varied to investigate the influence of much higher or much lower strength (and more economical) grout on strength and bond-slip response.
- 4.) A limited number of different bar sizes should be investigated.

- 5.) All future test specimens should have a slip wire attached to the free end of each bar to better monitor slip of the bars. Some use of strain gages on bars may also be advantageous to more closely monitor the bar strain.
- 6.) Some specimens should be subjected to a cyclic load history to investigate the utility of confined lap-splice connections for the use in design of precast seismic resistant buildings.

APPENDIX
EXPERIMENTAL DATA

Table A.1 Load-Deformation Response Data - #6 Bar - 12" Lap Length

Applied Load (kips)	Deformation Live End (inch x 10⁻³)	Deformation Dead End (inch x 10⁻³)	Comments
1	0.0	0.0	
2	0.0	1.0	
3	1.0	1.5	
4	2.0	2.0	
5	3.0	3.0	
6	4.0	3.5	
7	5.0	4.0	
8	5.5	5.0	
9	7.0	5.5	
10	8.0	6.0	
11	9.5	7.0	
12	10.5	8.0	
13	11.5	9.0	
14	12.5	10.0	
15	13.5	11.5	
16	14.0	13.0	
17	15.0	15.0	
18	18.0	16.5	
19	20.5	19.0	
20	23.0	21.0	
21	26.5	23.5	
22	29.5	26.0	
23	34.0	29.0	
24	38.0	31.5	

Table A.1 cont.

Applied Load (kips)	Deformation Live End (inch x 10 ⁻³)	Deformation Dead End (inch x 10 ⁻³)	Comments
25	43.0	34.0	
26	48.5	38.0	
27	53.5	41.0	
28	55.0	47.0	Yield = 28.1 k
29	123.0	61.5	
30	133.0	69.0	
31	141.0	74.0	
32	151.0	80.0	
33	161.0	84.0	
34	174.0	95.5	
35	190.5	135.0	1.25 Yield = 35.1 k
36	206.0	145.0	
37	222.5	169.0	1.32 Yield

Table A.2 Load-Deformation Response Data - #6 Bar - 15" Lap Length

Applied Load (kips)	Deformation Live End (inch x 10⁻³)	Deformation Dead End (inch x 10⁻³)	Comments
1	0.0	0.0	
2	0.0	0.5	
3	0.0	1.0	
4	0.5	1.5	
5	1.0	2.0	
6	1.5	2.5	
7	2.0	3.0	
8	2.5	3.5	
9	3.0	4.0	
10	3.5	4.5	
11	4.0	5.0	
12	5.0	5.5	
13	6.0	6.0	
14	6.5	6.5	
15	7.0	7.0	
16	8.0	7.5	
17	9.0	8.0	
18	9.5	8.5	
19	10.0	9.0	
20	11.5	10.0	
21	12.5	11.5	
22	14.0	13.0	
23	15.0	15.0	
24	17.0	17.0	

Table A.2 cont.

Applied Load (kips)	Deformation Live End (inch x 10⁻³)	Deformation Dead End (inch x 10⁻³)	Comments
25	18.0	19.0	
26	20.0	22.0	
27	23.0	25.5	
28	39.0	28.0	Yield = 28.1 k
29	47.0	50.5	
30	50.0	58.0	
31	58.0	68.0	
32	77.0	77.0	
33	92.0	85.0	
34	111.0	97.5	
35	133.0	111.0	1.25 Yield = 35.1 k
36	143.0	125.0	
37	157.0	141.0	1.32 Yield

Table A.3 Load-Deformation Response Data - #6 Bar - 19" Lap Length

Applied Load (kips)	Deformation Live End (inch x 10⁻³)	Deformation Dead End (inch x 10⁻³)	Comments
1	0.0	0.0	
2	0.0	0.5	
3	1.0	1.0	
4	1.5	1.5	
5	2.0	2.0	
6	2.5	2.5	
7	3.0	3.0	
8	3.5	3.5	
9	4.0	4.0	
10	4.5	4.5	
11	5.0	5.0	
12	5.5	5.5	
13	6.0	6.0	
14	6.5	6.5	
15	7.0	7.0	
16	7.5	7.5	
17	8.0	8.0	
18	8.75	8.5	
19	9.0	9.0	
20	10.0	9.75	
21	11.0	10.75	
22	12.0	11.5	
23	13.0	12.75	
24	14.0	13.75	

Table A.3 cont.

Applied Load (kips)	Deformation Live End (inch x 10 ⁻³)	Deformation Dead End (inch x 10 ⁻³)	Comments
25	15.0	14.75	
26	17.0	16.5	
27	21.0	20.5	
28	25.0	24.5	Yield = 28.1 k
29	50.0	48.5	
30	57.0	55.0	
31	66.0	64.5	
32	73.0	72.0	
33	81.0	78.5	
34	92.0	90.5	
35	105.0	102.0	1.25 Yield = 35.1 k
36	124.0	122.0	
37	140.0	139.0	1.32 Yield

Table A.4 Load-Deformation Response Data - #10 Bar - 24" Lap Length

Applied Load	Deformation Dead End (inch x 10⁻³)	Comments
0	0.0	Note: Live End Dial Gage Malfunction.
2	1.0	
4	3.0	
6	6.0	
8	8.0	
10	14.0	
12	16.0	
14	18.0	
16	22.0	
18	25.0	
20	28.0	
22	30.0	
24	33.0	
26	36.0	
28	38.0	
30	41.0	
32	43.0	
34	45.0	
36	46.0	
38	48.0	
40	49.0	
42	51.0	
44	53.0	
46	55.0	
48	58.0	

Table A.4 cont.

Applied Load (kips)	Deformation Dead End (inch x 10 ⁻³)	Comments
50	61.0	Note: Live End Dial Gage Malfunction.
52	64.0	
54	66.0	
56	70.0	
58	75.0	
60	80.0	
62	86.0	
64	93.0	
66	101.0	
68	111.0	
70	121.0	
72	130.0	
74	142.0	
76	153.0	
78	162.0	
80	170.0	
82	181.0	Yield = 82.5 k
84	208.0	
86	219.0	
88	228.0	
90	240.0	
92	253.0	
94	269.0	
96	283.0	
98	296.0	

Table A.4 cont.

Applied Load (kips)	Average Deformation (inch x 10⁻³)	Comments
100	312.0	Note: Live End Dial Gage Malfunction.
102	334.0	1.25 Yield = 103.1 k
104	359.0	
106	379.0	1.28 Yield

Table A.5 Load-Deformation Response Data - #10 Bar - 32" Lap Length

Applied Load (kips)	Deformation Live-End (inch x 10⁻³)	Deformation Dead-End (inch x 10⁻³)	Comments
0	0.0	0.0	
2	1.0	1.5	
4	1.5	2.5	
6	2.0	3.5	
8	2.5	4.5	
10	3.5	5.5	
12	4.0	6.5	
14	5.0	7.5	
16	6.0	9.0	
18	7.0	9.5	
20	8.0	10.0	
22	9.0	11.0	
24	10.0	12.0	
26	10.5	13.0	
28	11.0	14.0	
30	12.0	15.0	
32	13.0	16.0	
34	14.0	17.0	
36	14.5	18.0	
38	15.0	19.0	
40	16.0	20.0	
42	17.0	21.0	
44	18.0	22.0	
46	19.0	23.0	
48	20.0	24.0	

Table A.5 cont.

Applied Load (kips)	Deformation Live End (inch x 10 ⁻³)	Deformation Dead End (inch x 10 ⁻³)	Comments
50	21.0	25.0	
52	22.0	26.0	
54	22.5	27.0	
56	23.5	28.0	
58	25.0	29.0	
60	26.0	30.0	
62	27.5	31.0	
64	29.0	32.0	
66	30.5	33.0	
68	32.5	35.0	
70	34.5	37.0	
72	36.5	42.0	
74	39.0	45.0	
76	41.0	48.0	
78	43.0	52.0	
80	46.0	55.0	
82	49.0	57.0	Yield = 82.5 k
84	65.0	88.0	
86	94.0	99.0	
88	100.0	105.0	
90	109.0	116.0	
92	128.0	132.0	
94	142.0	145.0	
96	160.0	165.0	
98	171.0	177.0	

Table A.5 cont.

Applied Load (kips)	Deformation Live End (inch x 10⁻³)	Deformation Dead End (inch x 10⁻³)	Comments
100	185.0	192.0	
102	202.0	210.0	1.25 Yield = 103.1k
104	218.0	229.0	
106	234.0	245.0	1.28 Yield

Table A.6 Load-Deformation Response Data - #10 Bar - 41" Lap Splice

Applied Load (kips)	Deformation Live End (inch x 10⁻³)	Deformation Dead End (inch x 10⁻³)	Comments
0	0.0	0.0	
2	1.0	1.0	
4	2.0	2.0	
6	3.0	2.5	
8	5.0	4.0	
10	6.5	5.5	
12	8.0	7.0	
14	9.0	8.5	
16	10.0	9.5	
18	10.5	10.0	
20	11.5	10.5	
22	12.0	11.0	
24	13.5	12.0	
26	14.0	13.0	
28	15.0	14.0	
30	16.0	15.0	
32	17.0	16.0	
34	18.5	17.0	
36	19.5	18.0	
38	20.5	19.0	
40	21.5	20.0	
42	22.75	21.0	
44	24.0	22.0	
46	25.0	23.0	
48	26.0	24.0	

Table A.6 cont.

Applied Load (kips)	Deformation Live End (inch x 10 ⁻³)	Deformation Dead End (inch x 10 ⁻³)	Comments
50	27.0	25.0	
52	28.0	26.0	
54	29.0	27.0	
56	30.5	29.0	
58	31.5	30.5	
60	32.5	32.0	
62	34.0	33.0	
64	35.0	34.0	
66	36.5	35.0	
68	38.0	36.5	
70	40.0	38.0	
72	43.0	40.0	
74	44.0	42.0	
76	49.0	45.0	
78	51.5	47.5	
80	54.0	50.0	
82	58.0	54.0	Yield = 82.5k
84	87.0	84.0	
86	90.0	88.0	
88	101.0	99.0	
90	113.0	110.0	
92	123.0	121.0	
94	135.5	133.0	
96	146.5	144.0	
98	155.0	154.0	

Table A.6 cont.

Applied Load (kips)	Deformation Live End (inch x 10⁻³)	Deformation Dead End (inch x 10⁻³)	Comments
100	169.0	166.0	
102	184.0	180.0	1.25 Yield = 103.1k
104	199.5	194.0	
106	215.5	209.0	1.28 Yield

REFERENCES

1. ACI Committee 318, "Building Code Requirements for Reinforced Concrete and Commentary," ACI Standard 318-89, American Concrete Institute, Detroit, Michigan, 1989.
2. ACI Committee 201, "Durability of Concrete in Service," Journal of the American Concrete Institute, Proc. Vol. 59, No. 12, December 1962, pp. 1796-1801.
3. ACI Committee 408, "Bond Stress - The State of the Art," Journal of the American Concrete Institute, Vol. 63, November 1966.
4. American Institute of steel Construction, "Manual of Steel Construction - Allowable Stress Design," Ninth Edition, Chicago, Ill., 1988.
5. American Institute of Steel Construction, "Manual of Steel Construction - Load and Resistance Factor Design," Second Edition, Chicago, Ill., 1990.
6. Burns, N.H., "The Efficiency of Spiral Reinforcement Around Lapped Splices in Reinforced Concrete Beams," MS Thesis Department of Structural Engineering, School of Architectural Engineering, The University of Texas at Austin, August 1958.
7. Campi, V., Eligehausen, R., Bertero, V.V., Popov, E.P., "Analytical Model for Concrete Anchorages of Reinforcing Bars Under Generalized Excitations," EERC Report No. UCB/EERC-82/23, College of Engineering, The University of California at Berkeley, November 1982.
8. DeVries, R.A., and Moehle, J.P., "Lap Splice Strength of Plain and Epoxy-Coated Reinforcement," Department of Structural Engineering, Mechanics and Materials, School of Civil Engineering, University of California at Berkeley, 1989, pp. 117.

9. Eligehausen, R., Popov, E.P., Bertero, V.V., "Local Bond Stress-Slip Relationships of Deformed Bars Under Generalized Excitations," EERC Report No. UCB/EERC-83/23, College of Engineering, The University of California at Berkeley, October 1983.
10. Guimaraes, G.N., "Reinforced Concrete Frame Connections Constructed Using High Strength Materials," PhD Dissertation, Department of Civil Engineering, The University of Texas at Austin, December 1988pp.16.
11. Hamad, B.S., "Effect of Epoxy Coating on Bond and Anchorage of Reinforcement in Concrete Structures," PhD Dissertation, Department of Civil Engineering, The University of Texas at Austin, December 1990, pp. 20-28.
12. Luke, J.J., Hamad, B.S., Jirsa, J.O., and Breen, J.E., "The Influence of Casting Position on Development and Splice Length of Reinforcement," Research Report 242-1, Center for Transportation Research, The University of Texas at Austin, June 1981, pp. 115.
13. Lutz, L.A., Gergley, P., and Winter, G., "The Mechanics of Bond and Slip of Deformed Reinforcing Bars in Concrete," Department of Structural Engineering, School of Civil Engineering, Cornell University, Report No. 324, Ithaca, New York, August 1966, pp. 300.
14. Orangun, C.O., Jirsa, J.O., and Breen, J.E., "The Strength of Anchored Bars: A Reevaluation of Test Data on Development Length and Splices," Research Report 154-3F, Center for Highway Research, The University of Texas at Austin, January 1975.
15. Prestressed Concrete Institute, "Connections for Precast Prestressed Concrete Buildings Including Earthquake Resistance," PCI, Chicago, Illinois, March 1982.
16. Post-Tensioning Institute, "Post-Tensioning Manual", PTI, Phoenix, Arizona, Fifth Edition, 1990.

17. Rezansoff, T., "The Performance of Lapped Splices in Reinforced Concrete Under Rapid Loading," PhD Dissertation, Department of Civil Engineering, The University of Texas at Austin, May 1976.
18. Winter, G., Nilson, A.H., "Design of Concrete Structures," McGraw-Hill Book Company, Ninth Edition, New York, 1979.

VITA

John Joseph Myers was born in Reading, Pennsylvania, on July 27, 1964, the son of Anna Rosé Talarico Myers and Curvin Lee Myers Jr. After completing his work at Governor Mifflin High School, Shillington, Pennsylvania in 1982, he entered The Pennsylvania State University in State College, Pennsylvania. While participating in Varsity Track and Cross Country for Penn State, he was accepted into the Architectural Engineering Program in the College of Engineering with an emphasis in structural engineering during his sophomore year. Upon receiving the five-year professional degree of Bachelor of Architectural Engineering in May, 1987, he accepted a position as a structural design engineer with the internationally known AE Firm of RTKL Associates Inc., headquartered in Baltimore, Maryland. He spent approximately four years with the firm working on varied projects from high-rise office buildings to various retail and medical projects until accepting a project engineering position in April, 1991 with the Structural Engineering Consulting Firm of LPJ Inc., located in Baltimore, Maryland. In April of 1992 he sat and passed the Professional Engineers' Exam and became professionally registered in two states. In August, 1992, he entered The Graduate School of The University of Texas at Austin.

Permanent address: 7600 Wood Hollow Dr. #119
 Austin, Texas 78731-2242

This thesis was typed by John Joseph Myers.